

Impact of uncertainties of crustal model and source variability on ground motions

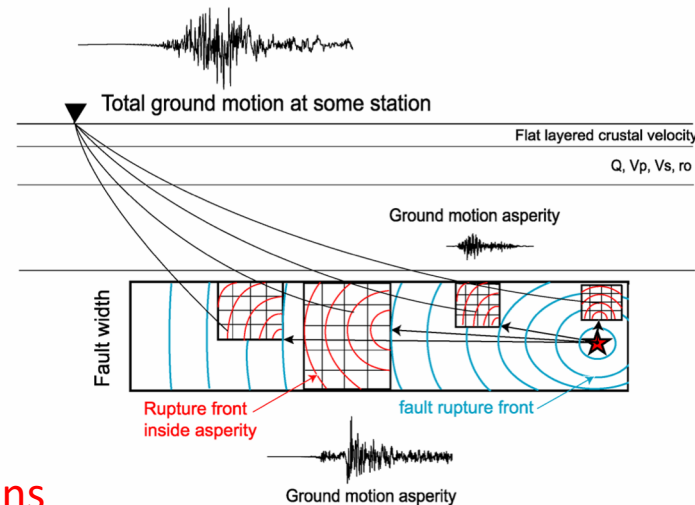
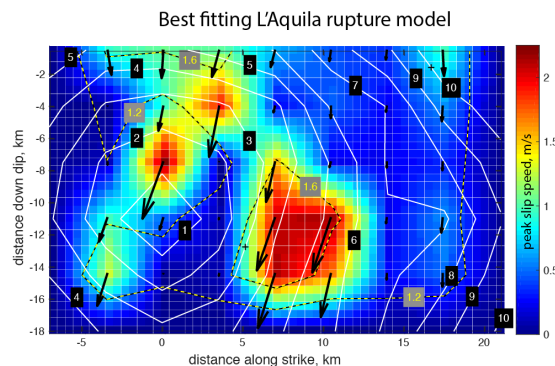
Elisa Tinti

Istituto Nazionale di Geofisica e Vulcanologia, Roma, Italy



ISTITUTO NAZIONALE
DI GEOFISICA E VULCANOLOGIA

Inferring earthquake source models is an essential ingredient in efforts to understand the physics of seismic rupture phenomena and the relationship of an earthquake with its tectonic and geodynamic environment. The earthquake source model is not only an end in itself but serves as input into a variety of other related applications such as earthquake energy budget, Coulomb stress calculations, seismic hazard, PGV estimates...



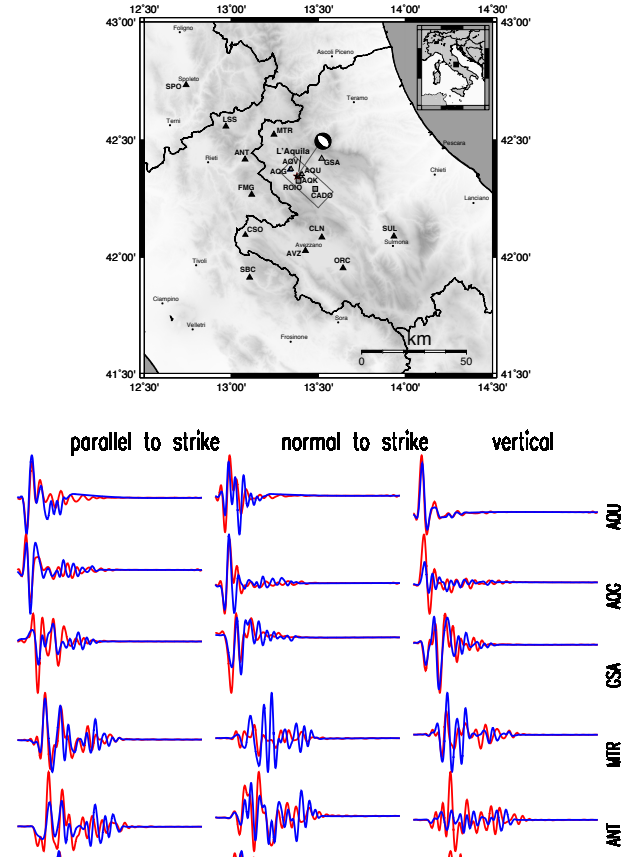
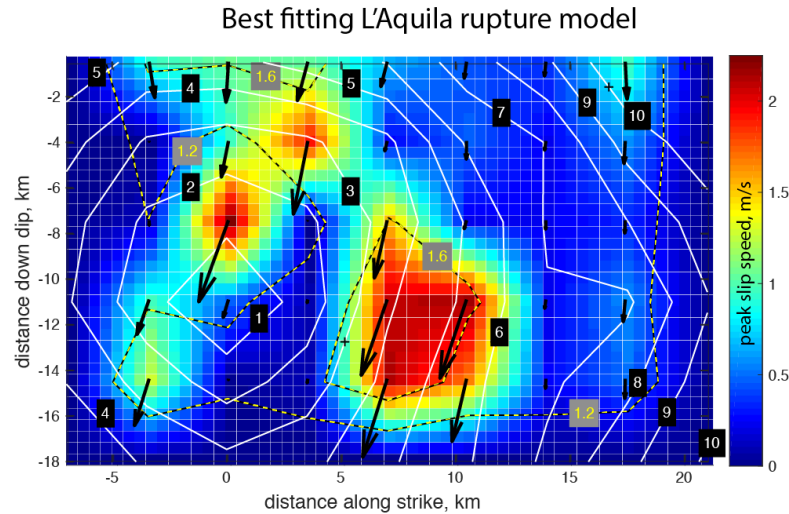
It is fundamental to find «reliable» solutions

However, source inversion algorithms usually do not include realistic error analyses and their results are generally not accompanied by reliable estimates of uncertainty. These limitations reduce the utility of inferred rupture models and associated by-products. Furthermore, uncertainty in both data and model predictions can cause current source models to be significantly biased due to **overfitting** of seismic and geodetic observations (Duputel et al. 2014).

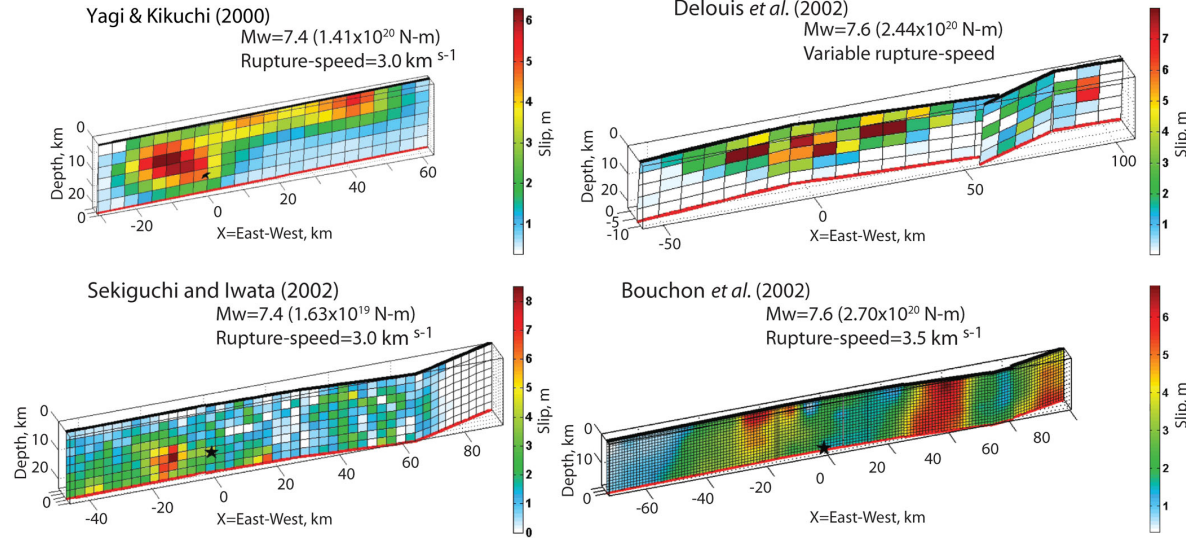
Overfit: to obtain an excessively good fit to the data considering the non-negligible errors. This meaning differs from the typical usage in statistics where overfit implies that a model has been overparametrized and fits noise as well as signal.

Introduction

Given a kinematic slip model and a local seismic velocity structure, it is straightforward to calculate the resulting ground motions deterministically.



Izmit 1999 earthquake source models



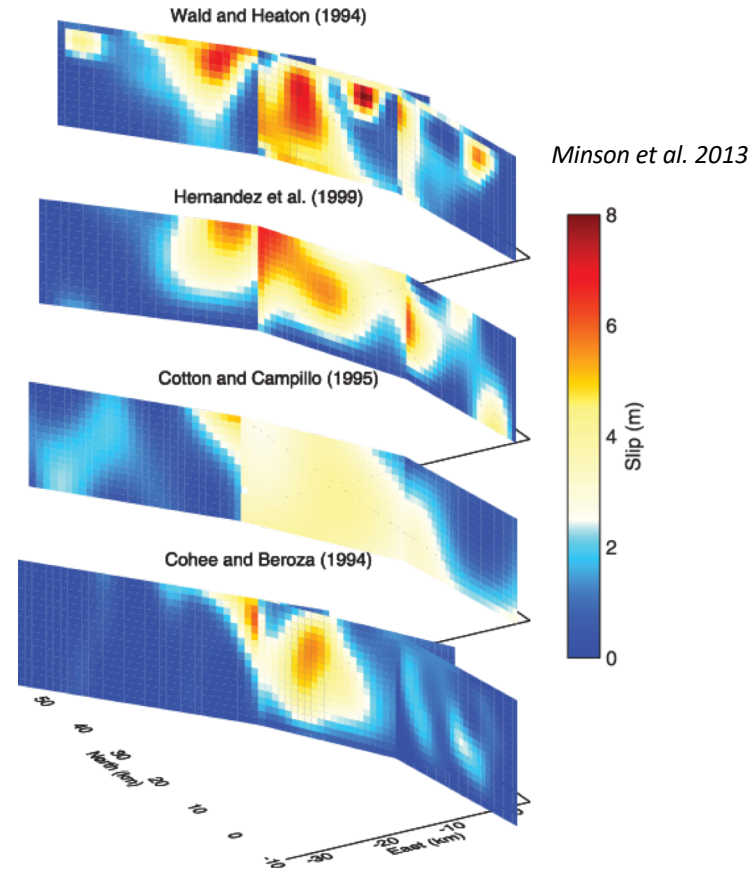
Duputel et al. 2014

The reliability of any source inversion depends on many factors including the size and complexity of the event, the amount and quality of data, the way in which data sample the source region and, while usually disregarded, uncertainties in our forward models (i.e. our model predictions).

We distinguish two sources of uncertainty:

the first class of error is induced by imperfect measurements and is often referred to as **observational error**.

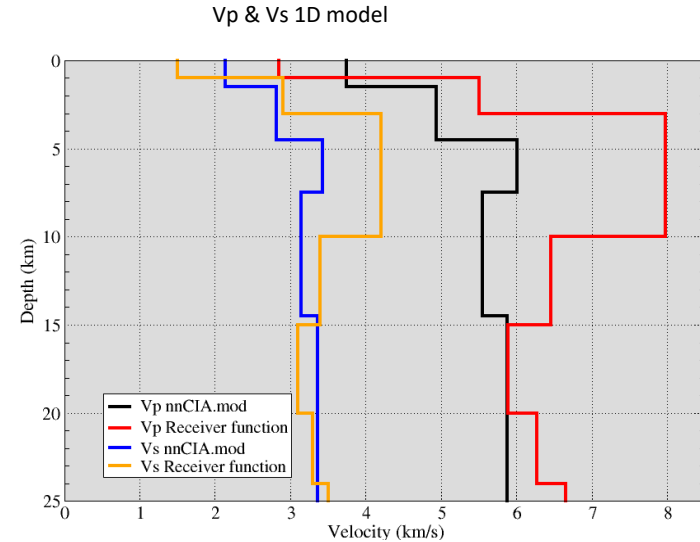
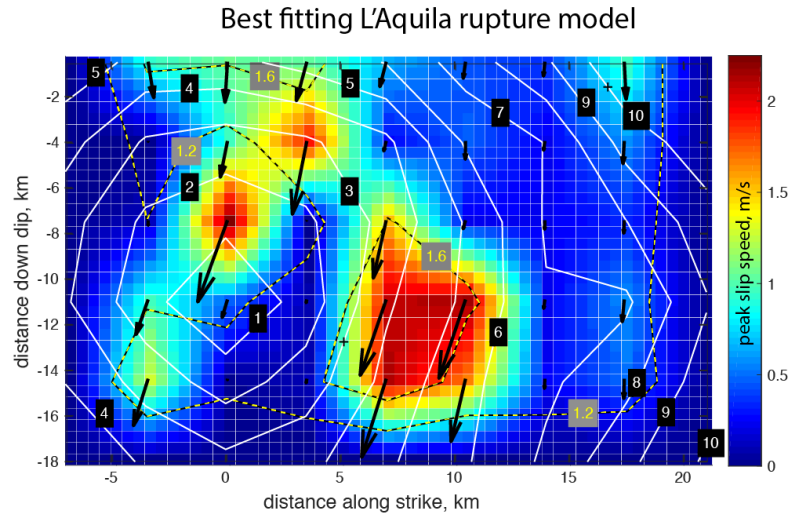
The second source of uncertainty is generally neglected and corresponds to the **prediction error**, that is the uncertainty due to imperfect forward modelling.



1992 Mw 7.3 Landers, California earthquake

Introduction

The prediction error is due to imperfect forward modelling, also referred to as **epistemic error**. For earthquake source modelling problems, this component includes but is not limited to, lack of fidelity in the fault geometry, **oversimplifications of the mechanical earth model** and approximations made when calculating the Earth's response to an applied force (**theory error**).



Example: during the forward modeling we have to assume some Earth structure (seismic velocities, density and anelastic attenuation) that is necessarily inaccurate (even if we use 1D models or 3D models).

LITERATURE –

- ✓ Recently Yagi and Fukahata (2011) presented a method to include uncertainties in Green functions (*theory errors*) into an inversion for earthquake rupture behavior, by using a time-domain approach. They were possibly the first investigators to try to quantify the variation of the ground motions caused by errors in the Green's function.
- ✓ *Theory errors* are also included in Bayesian inversion (Duputel et al (2012), Duputel et al. (2014), Minson et al (2013), Ragon et al. (2018)), by using a time-domain approach, through theoretical considerations.



Introduction of uncertainty of Green's function into waveform inversion for seismic source processes

Yuji Yagi¹ and Yukitoshi Fukahata²

¹*Graduate School of Life and Environmental Sciences, University of Tsukuba, Japan. E-mail: yagi-y@geol.tsukuba.ac.jp*

²*Disaster Prevention Research Institute, Kyoto University, Japan*

Accepted 2011 April 21. Received 2011 March 25; in original form 2010 November 15

SUMMARY

In principle, we can never know the true Green's function, which is a major error source in seismic waveform inversion. So far, many studies have devoted their efforts to obtain a Green's function as precise as possible. In this study, we propose a new strategy to cope with this problem. That is to say, we introduce uncertainty of Green's function into waveform inversion analyses. Due to the propagation law of errors, the uncertainty of Green's function results in a data covariance matrix with significant off-diagonal components, which naturally reduce the weight of observed data in later phases. Because the data covariance matrix depends on the model parameters that express slip distribution, the inverse problem to be solved becomes non-linear. Applying the developed inverse method to the teleseismic *P*-wave data of the 2006 Java, Indonesia, tsunami earthquake, we obtained a reasonable slip-rate distribution and moment-rate function without the non-negative slip constraint. The solution was independent of the initial values of the model parameters. If we neglect the modelling errors due to Green's function as in the conventional formulation, the total slip distribution is much rougher with significant opposite slip components, whereas the moment-rate function is much smoother. If we use a stronger smoothing constraint, more plausible slip distribution can be obtained, but then the moment-rate function becomes even smoother. By comparing the observed waveforms with the synthetic waveforms, we found that high-frequency components were well reproduced only by the new formulation. The modelling errors are essentially important in waveform inversion analyses, although they have been commonly neglected.

Yagi and Fukuhata 2011 introduce uncertainty of Green's function into waveform inversion analyses. They proposed a stochastic forward model (in terms of probability density function) based on adding Gaussian noise to the unattenuated 1-D teleseismic Green's functions. This Gaussian noise is characterized by a covariance matrix that is partially specified apriori. Due to the propagation law of errors, the uncertainty of Green's function results in a data **covariance matrix** with significant off-diagonal components whose elements **are proportional to the square of the maximum value of theoretical Green's functions**.

They apply this new methodology to the 2006 July 17 Java tsunami earthquake

Overfit: to obtain an excessively good fit to the data considering the non-negligible errors. This meaning differs from the typical usage in statistics where overfit implies that a model has been overparametrized and fits noise as well as signal.

Covariance: is a measure of the joint variability of two random variables.

Covariance matrix: is a matrix whose element in the i, j position is the covariance between the i -th and j -th elements of a random vector. Each element on the principal diagonal of the covariance matrix is the variance of one of the random variables

$$K_{X_i X_j} = \text{cov}[X_i, X_j] = \text{E}[(X_i - \text{E}[X_i])(X_j - \text{E}[X_j])]$$



Accounting for prediction uncertainty when inferring subsurface fault slip

Zacharie Duputel,^{1,*} Piyush S. Agram,^{1,†} Mark Simons,¹ Sarah E. Minson¹
and James L. Beck²

¹*Seismological Laboratory, California Institute of Technology, 1200 E California Blvd., Pasadena, CA 91125-2100, USA. E-mail: zacharie.duputel@unistra.fr*

²*Division of Engineering and Applied Science, California Institute of Technology, 1200 E California Blvd., Pasadena, CA 91125-2100, USA*

Accepted 2013 December 20. Received 2013 December 20; in original form 2013 August 1

SUMMARY

This study lays the groundwork for a new generation of earthquake source models based on a general formalism that rigorously quantifies and incorporates the impact of uncertainties in fault slip inverse problems. We distinguish two sources of uncertainty when considering the discrepancy between data and forward model predictions. The first class of error is induced by imperfect measurements and is often referred to as observational error. The second source of uncertainty is generally neglected and corresponds to the prediction error, that is the uncertainty due to imperfect forward modelling. Yet the prediction error can be shown to scale approximately with the size of earthquakes and thus can dwarf the observational error, particularly for large events. Both sources of uncertainty can be formulated using the misfit covariance matrix, C_χ , which combines a covariance matrix for observation errors, C_d and a covariance matrix for prediction errors, C_p , associated with inaccurate model predictions. We develop a physically based stochastic forward model to treat the model prediction uncertainty and show how C_p can be constructed to explicitly account for some of the inaccuracies in the earth model. Based on a first-order perturbation approach, our formalism relates C_p to uncertainties on the elastic parameters of different regions (e.g. crust, mantle, etc.). We demonstrate the importance of including C_p using a simple example of an infinite strike-slip fault in the quasi-static approximation. In this toy model, we treat only uncertainties in the 1-D depth distribution of the shear modulus. We discuss how this can be extended to general 3-D cases and applied to other parameters (e.g. fault geometry) using our formalism for C_p . The improved modelling of C_p is expected to lead to more reliable images of the earthquake rupture, that are more resistant to overfitting of data and include more realistic estimates of uncertainty on inferred model parameters.

Duputel et al 2014 provide a general formalism to explicitly quantify the impact of uncertainties in forward models and to rigorously incorporate such uncertainties in source inversion problems. They use a **stochastic forward modelling approach** that permits to describe a probability distribution of predictions for a given source model, contrary to a deterministic approach that provides a single set of predictions.

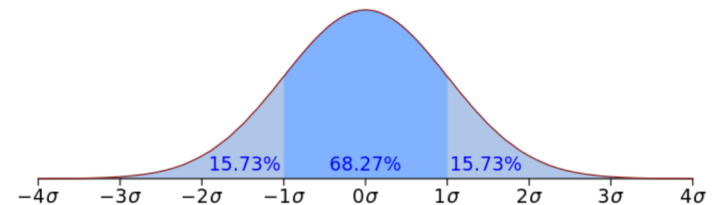
Dictionary:

Overfit: to obtain an excessively good fit to the data considering the non-negligible errors. This meaning differs from the typical usage in statistics where overfit implies that a model has been overparametrized and fits noise as well as signal.

Covariance: is a measure of the joint variability of two random variables.

Probability density function (PDF): is a function whose value at any given sample in the sample space can be interpreted as providing a relative likelihood that the value of the random variable would equal that sample.

The PDF is used to specify the probability of the random variable falling *within a particular range of values*.



Duputel et la 2014 quantify the impact of uncertainties (due to both observational error and prediction error) and incorporate such uncertainties in source inversion problems.

$$C\chi=C_d+C_p$$

Both sources of uncertainty can be formulated by use the misfit covariance matrix, C_χ , which combines a covariance matrix for observation errors, C_d and a covariance matrix for prediction errors, C_p , associated with inaccurate model predictions.

INVERSION PROCEDURE

They use a Bayesian inversion procedure in which they combine prior informations to construct a posterior distribution for source model parameters.

$$\chi(\mathbf{m}) = \frac{1}{2} \left[\mathbf{d}_{\text{obs}} - \mathbf{g}(\tilde{\Psi}, \mathbf{m}) \right]^T \cdot \mathbf{C}_\chi^{-1} \cdot \left[\mathbf{d}_{\text{obs}} - \mathbf{g}(\tilde{\Psi}, \mathbf{m}) \right].$$

$$p(\mathbf{d}_{\text{obs}}|\mathbf{m}) = \eta(\mathbf{m})\exp (- \chi(\mathbf{m})).$$

by defining a least-squares misfit function the likelihood function depends on C_χ

\mathbf{C}_d observational error $e = d - d^*$

The probability density function (PDF) for the observational error (stochastic model) is assumed to be a Gaussian with Covariance matrix \mathbf{C}_d and mean zero.

A common model is to take independent observational errors (i.e. diagonal \mathbf{C}_d). However, for observations like InSAR, off-diagonal components should be included in \mathbf{C}_d to allow correlation of measurement errors between neighboring data samples.

 \mathbf{C}_p prediction error $\epsilon = d - d_{pred}$

The PDF for the prediction error (stochastic forward model) describes the uncertainty in the actual physical quantity \mathbf{d} given \mathbf{d}_{pred} and is assumed to be Gaussian with Covariance matrix \mathbf{C}_p and mean zero. This error scales approximately with the size of earthquakes and, for large events, the contribution of \mathbf{C}_d is thus frequently negligible compared to \mathbf{C}_p .

Why does C_p error scale approximately with the size of earthquakes?

$g(\Psi, m)$ is a deterministic model for a source model m and Ψ represents a set of uncertain properties (e.g., rigidity, density, fault geometry...):

$$\epsilon = d - d_{pred} = d - g(\tilde{\Psi}, m)$$

where $\tilde{\Psi}$ represents the most plausible value a priori (*erroneous*).

If we consider the linear formulation of the forward problem $g(\Psi, m) = G(\Psi) \cdot m$

Therefore we can write:

$$\epsilon = d - d_{pred} = g(\Psi, m) - g(\tilde{\Psi}, m) = [G(\Psi) - G(\tilde{\Psi})] \cdot m$$

How do they design a prediction covariance matrix C_p ?

If the uncertainty is due to a specific parameter Ψ (like the rigidity) after many equations Duputel et al. 2014 found that:

$$\mathbf{C}_p = \mathbf{K}_\Psi \cdot \mathbf{C}_\Psi \cdot \mathbf{K}_\Psi^T,$$

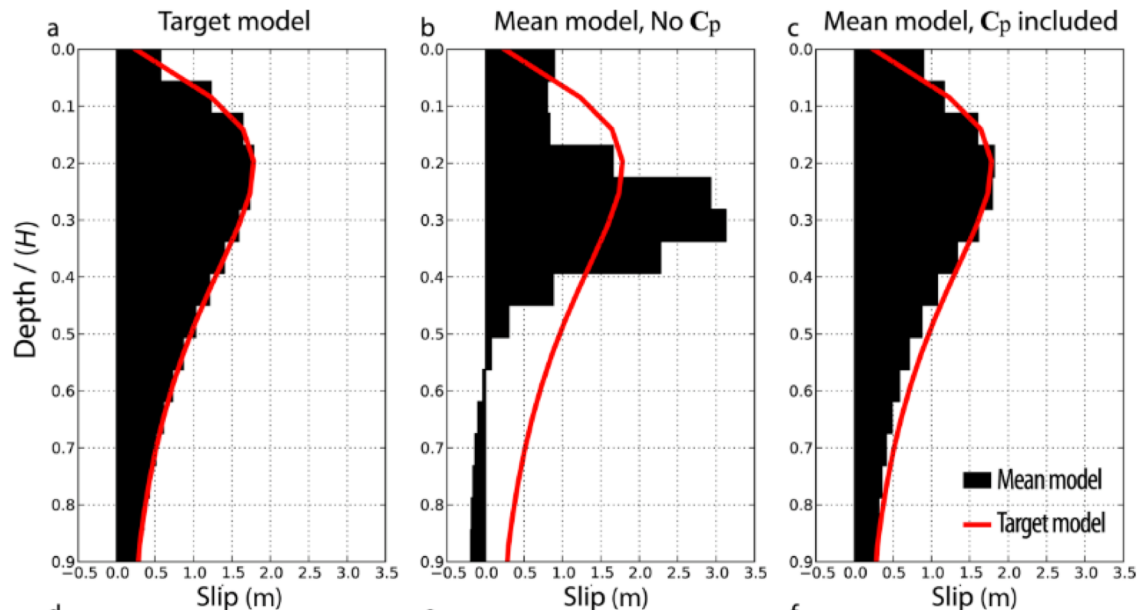
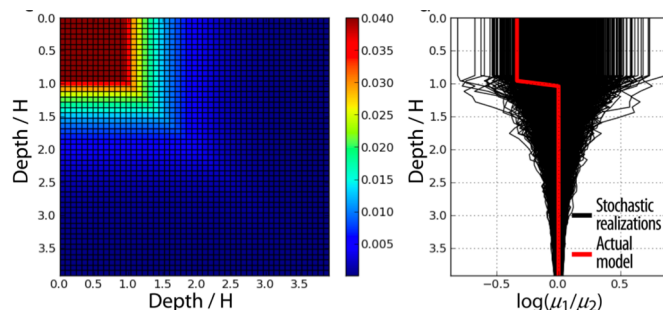
where C_Ψ represents the covariance matrix of that parameter and K_Ψ represents a kernel (that is the partial derivative of the model respect to that parameter). Duputel et al. 2014 **assume** that the prior probability density describing the uncertainty of the parameters Ψ follows a Gaussian distribution and its covariance matrix C_Ψ is:

$$\mathbf{C}_\Psi = \int (\Psi - \tilde{\Psi})(\Psi - \tilde{\Psi})^T p(\Psi) d\Psi.$$

This covariance matrix is built through a large number (> 1000) of stochastic earth model realizations.

How to use these information on the uncertainties during the kinematic rupture inversions?

Example: Bayesian inference to infer the static slip distribution from geodetic data in a vertically varying medium.



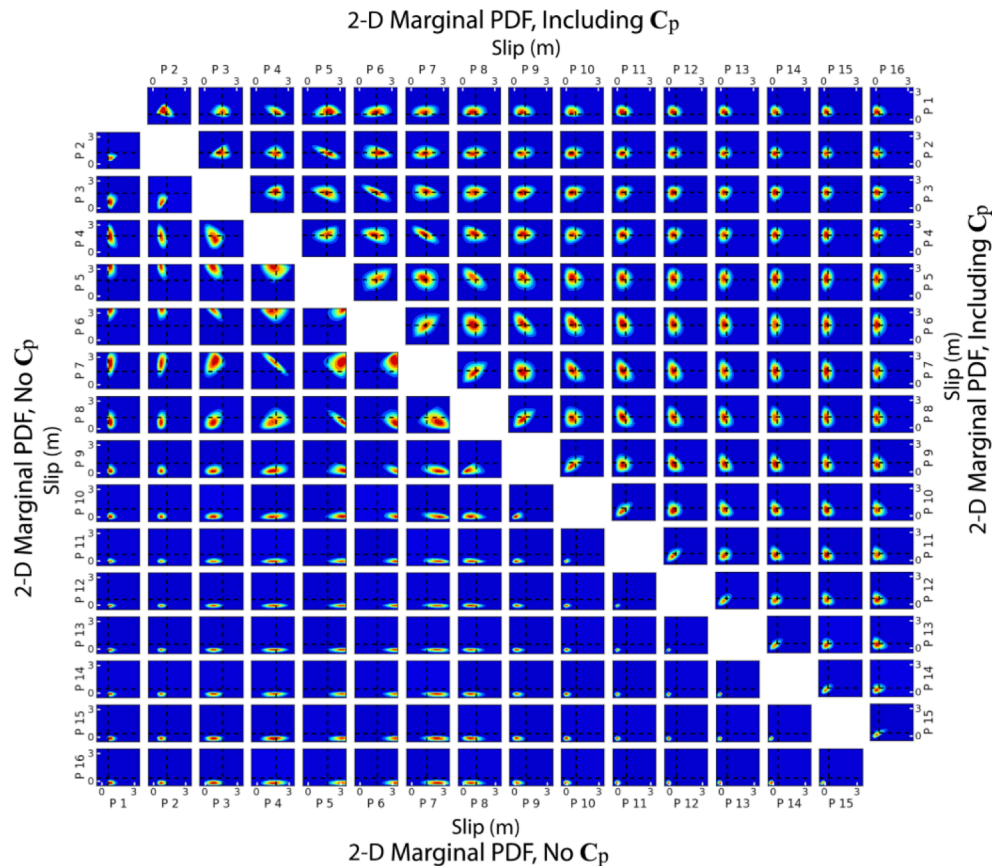
1000 stochastic realizations considering the layer thickness and shear modulus uncertain

The mean of the posterior distributions are shown in black

How to use these information on the uncertainties during the kinematic rupture inversions?

Marginal posterior probability densities for all possible pairs of fault patches. Numbers increase as a function of depth.

These PDF show very narrow peaks at large depth that are clearly shifted with respect to the target slip values. If C_p is included, they obtain much broader posterior distributions centred around a mean model that is in agreement with the target slip model



How to use these information on the uncertainties during the kinematic rupture inversions?

They recognize that their prediction covariance matrix C_p should also depend on the earthquake source model and is not just a constant matrix, that is, changing the magnitude and distribution of fault slip will change C_p for a given elastic model.

For practical implementation, there are different ways of dealing with the dependence of C_p upon the source model m . They test two ways:

- 1) They calculate $C_p(m_{\text{prior}})$ using an apriori source model, m_{prior} , such as a preliminary finite-fault model and assume that C_p is constant.
- 2) They propose to update the prediction covariance iteratively during the source inversion process.

LITERATURE –

- ✓ Recently Yagi and Fukahata (2011) presented a method to include uncertainties in Green functions (*theory errors*) into an inversion for earthquake rupture behavior, by using a time-domain approach. They were possibly the first investigators to try to quantify the variation of the ground motions caused by errors in the Green's function.
- ✓ *Theory errors* are also included in Bayesian inversion (Duputel et al (2012), Minson et al (2014), Ragon et al. (2018)) through theoretical considerations.

None of the investigators actually measured Green's function errors.

GOAL:

We want to compute the impact of uncertainties of crustal model and we derive the covariance matrix by **measuring** Green's function errors.

OUTLINES -

- 1) Present an equation of ground velocity that includes the **Green function errors** (frequency domain);
- 2) Derive the expected variance γ^2 caused by Green function errors for a large earthquake;
- 3) Compute the **Green function errors** for a test case (L'Aquila region);
- 4) Compare these errors with the misfit of the best model for the 2009 L'Aquila event, Mw 6.1;
- 5) General discussion on source variabilities and green functions errors;
- 6) Future applications.

All the results presented in the following slides come from:

The screenshot shows the article page on the Oxford Academic website. The header includes the Oxford Academic logo and the journal title 'Geophysical Journal International'. A navigation bar contains links for Issues, Subject, Advance articles, Submit, Purchase, and About. The article title is 'Variability in synthetic earthquake ground motions caused by source variability and errors in wave propagation models', marked as an 'ACCEPTED MANUSCRIPT' and 'FREE'. The authors listed are Paul Spudich, Antonella Cirella, Laura Scognamiglio, and Elisa Tinti. The publication details include 'Geophysical Journal International, ggz275' and a DOI link. The publication date is '24 June 2019'. Below the title, there are icons for PDF, Split View, Cite, Permissions, and Share. The 'Summary' section begins with the text: 'Numerical simulations of earthquake ground motions are used both to anticipate the effects of hypothetical earthquakes by forward simulation and to infer the behavior of the real earthquake source ruptures by inversion of recorded ground motions. In either application it is necessary to assume some Earth structure that is necessarily inaccurate and to use a computational method that is also inaccurate for simulating the wave field Green's functions. We refer to these two sources of error as 'propagation inaccuracies,' which

OXFORD
ACADEMIC

Geophysical Journal International

Issues ▾ Subject Advance articles Submit ▾ Purchase About ▾ All Geophysical Journal Int ▾

Article Contents

Summary

Notes

ACCEPTED MANUSCRIPT

Variability in synthetic earthquake ground motions caused by source variability and errors in wave propagation models ^{FREE}

Paul Spudich ✉, Antonella Cirella, Laura Scognamiglio, Elisa Tinti

Geophysical Journal International, ggz275, <https://doi.org/10.1093/gji/ggz275>

Published: 24 June 2019

PDF Split View Cite Permissions Share ▾

Summary

Numerical simulations of earthquake ground motions are used both to anticipate the effects of hypothetical earthquakes by forward simulation and to infer the behavior of the real earthquake source ruptures by inversion of recorded ground motions. In either application it is necessary to assume some Earth structure that is necessarily inaccurate and to use a computational method that is also inaccurate for simulating the wave field Green's functions. We refer to these two sources of error as 'propagation inaccuracies,' which

A major problem is that we do not know the seismic velocity structure perfectly and our methods for calculating traction Green's functions are inaccurate.

Let the true tractions on a fault at point caused by a point force in the j -direction at the observer at \mathbf{y} be $\mathbf{g}^{(j)}(\mathbf{x}, \omega; \mathbf{y})$

Let its numerical approximation based on an inaccurate velocity structure be $\tilde{\mathbf{g}}^{(j)}(\mathbf{x}, \omega; \mathbf{y})$

Let its error be $\delta \mathbf{g}^{(j)}(\mathbf{x}, \omega; \mathbf{y})$

so we have... $\mathbf{g}^{(j)}(\mathbf{x}, \omega; \mathbf{y}) = \tilde{\mathbf{g}}^{(j)}(\mathbf{x}, \omega; \mathbf{y}) + \delta \mathbf{g}^{(j)}(\mathbf{x}, \omega; \mathbf{y})$

Similarly, the relation between the true slip velocity, the assumed and the variation in slip velocity can be written:

$$\mathbf{s}(\mathbf{x}, \omega) = \mathbf{s}(\mathbf{x}, \omega) + \delta \mathbf{s}(\mathbf{x}, \omega)$$

Ground velocity in frequency domain:

$$d_j(\omega, \mathbf{y}) = v_j(\omega, \mathbf{y}) + n_j(\omega, \mathbf{y}).$$

Noise-free Ground velocity:

$$v_j(\omega, \mathbf{y}) = \int_{\mathbf{x} \in A} \mathbf{s}(\mathbf{x}, \omega) \cdot \mathbf{g}^{(j)}(\mathbf{x}, \omega; \mathbf{y}) dA$$

$v_j(\omega, \mathbf{y})$ is the Fourier Transform of the j component of ground velocity at location \mathbf{y}


$\mathbf{s}(\mathbf{x}, \omega)$ is the Fourier Transform of the slip velocity vector at location \mathbf{x}

$$= \int_{\mathbf{x} \in A} \mathbf{s} \cdot \mathbf{g}^{(j)} dA + \int_{\mathbf{x} \in A} \delta \mathbf{s} \cdot \mathbf{g}^{(j)} dA + \int_{\mathbf{x} \in A} \mathbf{s} \cdot \delta \mathbf{g}^{(j)} dA + \int_{\mathbf{x} \in A} \delta \mathbf{s} \cdot \delta \mathbf{g}^{(j)} dA.$$

Ground velocity in frequency domain


$$v_j(\omega, \mathbf{y}) = \int_{\mathbf{x} \in A} \mathbf{s} \cdot \mathbf{g}^{(j)} dA + \int_{\mathbf{x} \in A} \delta \mathbf{s} \cdot \mathbf{g}^{(j)} dA + \int_{\mathbf{x} \in A} \mathbf{s} \cdot \delta \mathbf{g}^{(j)} dA + \int_{\mathbf{x} \in A} \delta \mathbf{s} \cdot \delta \mathbf{g}^{(j)} dA.$$

δv_j^s



is a measure of the aleatory variability in the ground velocity caused by rupture source variability.

δv_j^g



is a measure of the epistemic variability in the ground velocity because errors in the geologic structure.

δv_j^{sg}



is the ground velocity caused by the interaction of $\delta \mathbf{g}$ and $\delta \mathbf{s}$. it might not be negligible depending on the amplitudes of $\delta \mathbf{s}$ and $d\delta$.

These terms show how variations in the rupture model and errors in the Green's functions contribute to the total motion.

Ground velocity in frequency domain

$$v_j(\omega, \mathbf{y}) = \int_{\mathbf{x} \in A} \mathbf{s} \cdot \mathbf{g}^{(j)} dA + \int_{\mathbf{x} \in A} \delta \mathbf{s} \cdot \mathbf{g}^{(j)} dA + \int_{\mathbf{x} \in A} \mathbf{s} \cdot \delta \mathbf{g}^{(j)} dA + \int_{\mathbf{x} \in A} \delta \mathbf{s} \cdot \delta \mathbf{g}^{(j)} dA.$$

 δv_j^s  δv_j^g δv_j^{sg}

I will show you how errors in the Green's functions contribute to the total motion

The variation in ground velocity caused by errors in our Green's function is

$$\delta v_j^g = \int_{\mathbf{x} \in A} \tilde{\mathbf{s}} \cdot \delta \mathbf{g}^{(j)} dA$$

We compute the variance of γ^2 of this term δv^g that can be related to the statistics of the Green's function error. This variance is a function of frequency, component and observation location.

Ground velocity in frequency domain:

$$d_j(\omega, \mathbf{y}) = \int_{\mathbf{x} \in A} \mathbf{s} \left[\mathbf{g}^{(j)} + \delta \mathbf{g}^{(j)} \right] dA + n_j(\omega, \mathbf{y}).$$

The slip velocity function

$$\mathbf{s}(\mathbf{x}, \omega) = \sum_{q=1}^2 a_q(\mathbf{x}) \hat{\mathbf{e}}_q T(\mathbf{x}, \omega) \exp(-i\omega t(\mathbf{x}))$$

$$d_j(\omega) = \sum_q \sum_k a_{qk} T(\omega) e^{-i\omega t_k} \left[G_{qkj}(\omega) + \delta G_{qkj}(\omega) \right] + n_j(\omega).$$

$u(\omega)$

By using the multidimensional delta method,
Considering the function $u(\omega)$ (Papanicolaou, 2016)

A Taylor expansion about $\mathbf{X} = \boldsymbol{\mu}$ gives

$$u(\mathbf{X}) \approx u(\boldsymbol{\mu}) + (\nabla u(\boldsymbol{\mu}))^T (\hat{\mathbf{X}} - \boldsymbol{\mu}).$$

If the function has continuous partial derivatives, then

$$\sqrt{N} \left(u(\hat{\mathbf{X}}) - u(\boldsymbol{\mu}) \right) \xrightarrow{D} N(0, \tau^2)$$

where $N(0, \tau^2)$ is the normal distribution with zero mean and variance τ^2 , which is given by

$$\tau^2 = (\nabla u(\boldsymbol{\mu}))^T \mathbf{C} \nabla u(\boldsymbol{\mu}).$$

Covariance matrix is a $P \times P$ matrix with elements

$$C_{ij} = E \left[(X_i^{(n)} - \mu_i) (X_j^{(n)} - \mu_j) \right]$$

$$d_j(\omega) = \sum_q \sum_k \underbrace{a_{qk} T(\omega) e^{-i\omega t_k} [G_{qkj}(\omega) + \delta G_{qkj}(\omega)]}_{u(\omega)} + n_j(\omega).$$

By using the multidimensional delta method, the variance of $u(\omega)$ (Papanicolaou, 2016)

$$\gamma_j^2 = \nabla \mathbf{u}_j^\dagger \mathbf{C}_j \nabla \mathbf{u}_j$$

where the dagger connotes complex-conjugate transpose.

and

$$\nabla \mathbf{u}_j = \left[\frac{\partial u_j}{\partial G_{1j}} \quad \frac{\partial u_j}{\partial G_{2j}} \quad \frac{\partial u_j}{\partial G_{pj}} \right]^T = [A_1 \ A_2 \ A_p]^T$$

the covariance is:

$$C_{prj} = E \left[\left(G_{pj} - G_{pj} \right)^* \left(G_{rj} - G_{rj} \right) \right] = E \left[\delta G_{pj}^* \delta G_{rj} \right]$$

$$A_{qk}(\omega) := a_{qk} T(\omega) B(\omega) e^{-i\omega t_k}$$

A_{qk} is the source term filtered with operator $B(\omega)$

$$\gamma_j^2 = \nabla \mathbf{u}_j^\dagger \mathbf{C}_j \nabla \mathbf{u}_j$$

Then for a particular source \tilde{s} , the variance is:

$$\gamma_j^2(\omega) = \int_{\mathbf{x} \in A} \int_{\mathbf{x}' \in A} \mathbf{s}^\dagger(\mathbf{x}, \omega) \mathbf{C}^j(\mathbf{x}, \mathbf{x}', \omega) \mathbf{s}(\mathbf{x}', \omega) d\mathbf{x} d\mathbf{x}'$$

Covariance of the Green's function errors between point \mathbf{x} and \mathbf{y}

$$\mathbf{C}^j(\mathbf{x}, \mathbf{y}, \omega) = E \left[\delta \mathbf{g}^{j*}(\mathbf{x}, \omega)^T \delta \mathbf{g}^j(\mathbf{y}, \omega) \right] = E \left[\begin{bmatrix} \delta g_1^j(\mathbf{x}) \\ \delta g_2^j(\mathbf{x}) \end{bmatrix}^* \begin{bmatrix} \delta g_1^j(\mathbf{y}) & \delta g_2^j(\mathbf{y}) \end{bmatrix} \right]$$

The general form is:

$$\gamma_j^2(\omega) = \int_{\mathbf{x} \subset A} \int_{\mathbf{x}' \subset A} \begin{bmatrix} s_1^*(\mathbf{x}) & s_2^*(\mathbf{x}) \end{bmatrix} \mathbf{C}^j(\mathbf{x}, \mathbf{x}') \begin{bmatrix} s_1(\mathbf{x}') \\ s_2(\mathbf{x}') \end{bmatrix} d\mathbf{x} d\mathbf{x}'$$

$$\mathbf{C}^j(\mathbf{x}, \mathbf{x}', \omega) = E \begin{bmatrix} \delta g_1^{(j)*}(\mathbf{x}) \delta g_1^{(j)}(\mathbf{x}') & \delta g_1^{(j)*}(\mathbf{x}) \delta g_2^{(j)}(\mathbf{x}') \\ \delta g_2^{(j)*}(\mathbf{x}) \delta g_1^{(j)}(\mathbf{x}') & \delta g_2^{(j)*}(\mathbf{x}) \delta g_2^{(j)}(\mathbf{x}') \end{bmatrix}$$

We can simplify for the common case that the rake in an earthquake rupture is primarily unidirectional. We can simplify by choosing the \mathbf{e}_1 unit vector to be directed along the dominant slip direction and assuming that the other component of slip is negligible.

We further simplify by assuming that the \mathbf{e}_1 component of Green's function error is uncorrelated with the \mathbf{e}_2 component. So \mathbf{C}_j becomes diagonal.

Developing a frequency-domain equivalent to Yagi and Fukahata (2011) we discovered the following simple relation for the variance of the ground motion:

$$\gamma_j^2(\omega) = \int_{\mathbf{x} \in A} \int_{\mathbf{x}' \in A} s_1^*(\mathbf{x}, \omega) C_{11}^j(\mathbf{x}, \mathbf{x}', \omega) s_1(\mathbf{x}', \omega) d\mathbf{x} d\mathbf{x}'$$

$$\gamma_j^2(\omega)$$

is the variance in ground velocity of the j-th channel (single component of motion at a particular observation location)

$$s_1^*(\mathbf{x}, \omega)$$

is the complex conjugate of the slip velocity in the dominant slip direction (called the '1' direction) at point x on the fault

$$C_{11}^j(\mathbf{x}_1, \mathbf{x}_2, \omega) = E[\delta g_1^{j*}(\mathbf{x}_1) \delta g_1^j(\mathbf{x}_2)]$$

is the covariance of the errors in the traction Greens functions

Derived covariance function

$$C_{11}^j(\mathbf{x}_1, \mathbf{x}_2, \omega) = E\left[\delta g_1^{j*}(\mathbf{x}_1) \delta g_1^j(\mathbf{x}_2)\right]$$

C_{11}^j is the covariance of the errors in the traction Greens functions at location \mathbf{x}_1 on the rupture area A with the errors in the traction Green's functions at location \mathbf{x}_2 on the rupture area for the j -th data channel (single component of motion at a particular observation location).

This covariance function allows us to make realistic estimates of the variance based on observed data quantifying Green's function error.

A simple model for this covariance function might be a function of the separation between points \mathbf{x}_1 and \mathbf{x}_2 on the rupture surface, with or without some dependence on frequency. This is one way of quantifying the spatial heterogeneity.

$$C_{11}^j(\mathbf{x}_1, \mathbf{x}_2, \omega) = E\left[\delta g_1^{j*}(\mathbf{x}_1) \delta g_1^j(\mathbf{x}_2)\right]$$

Physically we might expect two different functional forms for the spatial covariance:

If it is **dominated by finite frequency effects**, we might expect that an element of the covariance of the Green's function errors might be

$$\mathbf{C}^j(\mathbf{x}_1, \mathbf{x}_2, \omega) \propto f(|\mathbf{x}_1 - \mathbf{x}_2|, \omega)$$

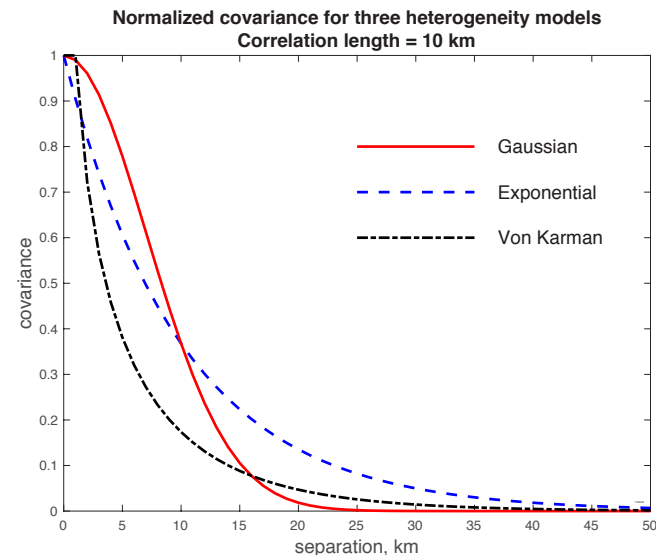
where f is some decreasing function like a Gaussian centered at the origin. In such a model the errors in the Green's functions would be correlated at progressively longer distances as the wavelengths of the shear wave increased.

Physically we might expect two different functional forms for the spatial covariance:

If it is dominated by finite frequency effects, we might expect that an element of the covariance of the Green's function errors might be

$$\mathbf{C}^j(\mathbf{x}_1, \mathbf{x}_2, \omega) \propto f(|\mathbf{x}_1 - \mathbf{x}_2|, \omega)$$

where f is some decreasing function like a Gaussian centered at the origin. In such a model the errors in the Green's functions would be correlated at progressively longer distances as the wavelengths of the shear wave increased.



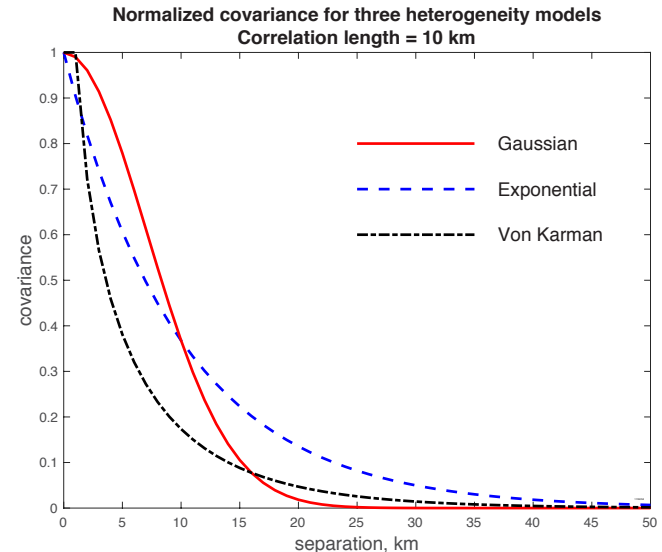
Physically we might expect two different functional forms for the spatial covariance:

If it is dominated by finite frequency effects, we might expect that an element of the covariance of the Green's function errors might be

$$C^j(\mathbf{x}_1, \mathbf{x}_2, \omega) \propto f(|\mathbf{x}_1 - \mathbf{x}_2|, \omega)$$

where f is some decreasing function like a Gaussian centered at the origin. In such a model the errors in the Green's functions would be correlated at progressively longer distances as the wavelengths of the shear wave increased.

On the other hand, if errors in the Green's functions are related to unmodeled spatial variations in the rigidity along the fault surface, this function might have **no frequency dependence**.



Finite Difference Simulations of Seismic Scattering;
Implications for the Propagation of Short-Period Seismic Waves
in the Crust and Models of Crustal Heterogeneity

ARTHUR FRANKEL
ROBERT W. CLAYTON

They used a 2D finite difference algorithm to model wave propagation in random heterogeneous media with three different autocovariance functions, a self-similar, an exponential, and a gaussian.

These media differ in the spectral falloff of their velocity fluctuations at wavelengths smaller than 2π times the correlation distance a .

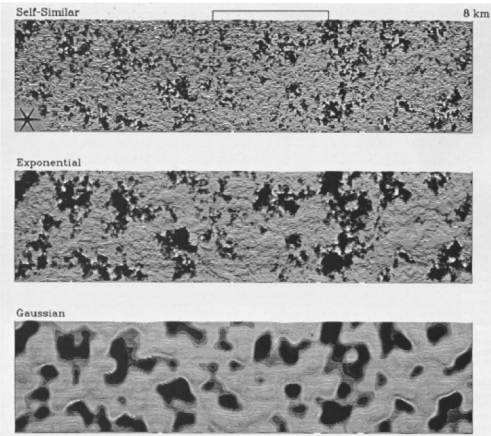


Fig. 1. Representations of the three types of random media considered in this study. Each medium shows has a correlation distance of 200 m. The amplitude of each horizontal line denotes the random component of the P or S wave velocity (V_p/V_s constant). Areas with higher than average velocity are shaded. In the top panel, the positions of the explosive source (star) and receiver array (line) along the free surface are shown. This configuration was used in the simulations described in the section on high-frequency coda amplitude and cross correlation.

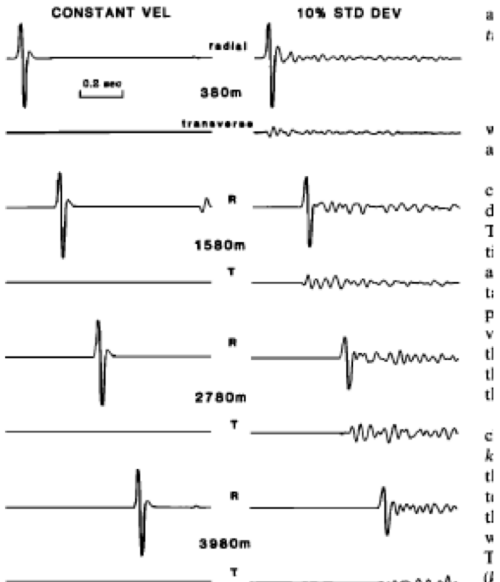


Fig. 4. (Left) Synthetic seismograms for a P wave propagating through a constant velocity medium (see Figure 2 for geometry). Radial and transverse components of velocity are shown for receivers from 380 to 3980 m from the source. Amplitudes of all synthetics shown in this paper are corrected for geometrical spreading. (Right) Synthetic seismograms for a P wave traveling through an exponential random medium ($\sigma_r = 10\%$, $a = 40$ m, $ka = 1.16$ at 30 Hz).

Finite Difference Simulations of Seismic Scattering;
Implications for the Propagation of Short-Period Seismic Waves
in the Crust and Models of Crustal Heterogeneity

ARTHUR FRANKEL
ROBERT W. CLAYTON

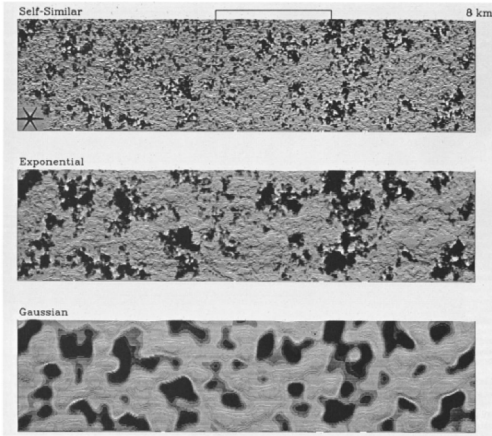
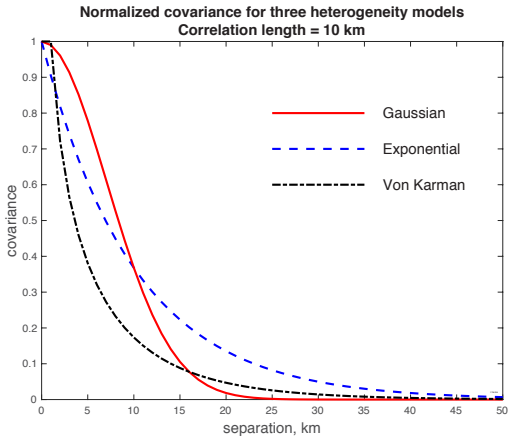


Fig. 1. Representations of the three types of random media considered in this study. Each medium shows a correlation distance of 200 m. The amplitude of each horizontal line denotes the random component of the P or S wave velocity (V_p/V_s constant). Areas with higher than average velocity are shaded. In the top panel, the positions of the explosion source (star) and receiver array (line) along the free surface are shown. This configuration was used in the simulations described in the section on high-frequency coda amplitude and cross correlation.

Frankel & Clayton (1986) specified the covariance of their random seismic velocity structures, and their variations in wave amplitude were the result of the random structures.

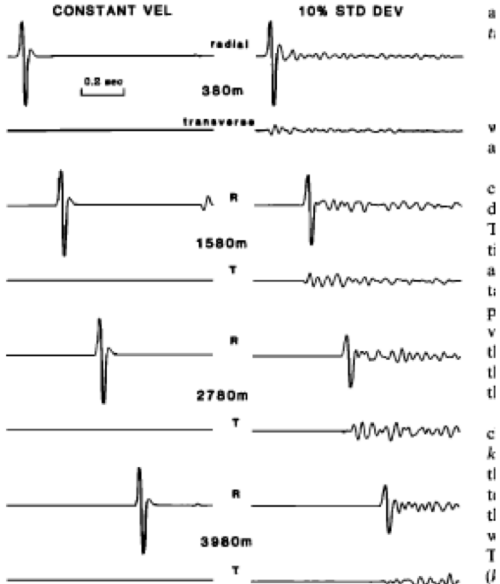


Fig. 4. (Left) Synthetic seismograms for a P wave propagating through a constant velocity medium (see Figure 2 for geometry). Radial and transverse components of velocity are shown for receivers from 380 to 3980 m from the source. Amplitudes of all synthetics shown in this paper are corrected for geometrical spreading. (Right) Synthetic seismograms for a P wave traveling through an exponential random medium ($\sigma_v = 10\%$, $a = 40$ m, $ka = 1.16$ at 30 Hz).

Finite Difference Simulations of Seismic Scattering;
Implications for the Propagation of Short-Period Seismic Waves
in the Crust and Models of Crustal Heterogeneity

ARTHUR FRANKEL
ROBERT W. CLAYTON

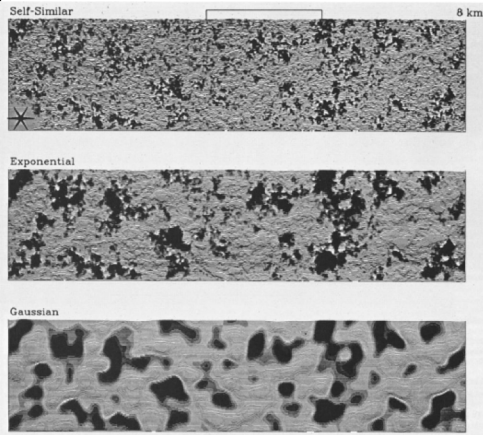


Fig. 1. Representations of the three types of random media considered in this study. Each medium shown has a correlation distance of 200 m. The amplitude of each horizontal line denotes the random component of the P or S wave velocity (V_p/V_s , constant). Areas with higher than average velocity are shaded. In the top panel, the positions of the explosion source (star) and receiver array (bar) along the free surface are shown. This configuration was used in the simulations described in the section on high-frequency coda amplitude and cross correlation.

They concluded that random media with **self-similar velocity fluctuations** with a correlation length of $a=10$ km can explain both teleseismic travel time anomalies and the presence of seismic coda at high frequencies

We, on the other hand, are using observations of aftershock seismograms to look directly at the random variation of the traction wave field.

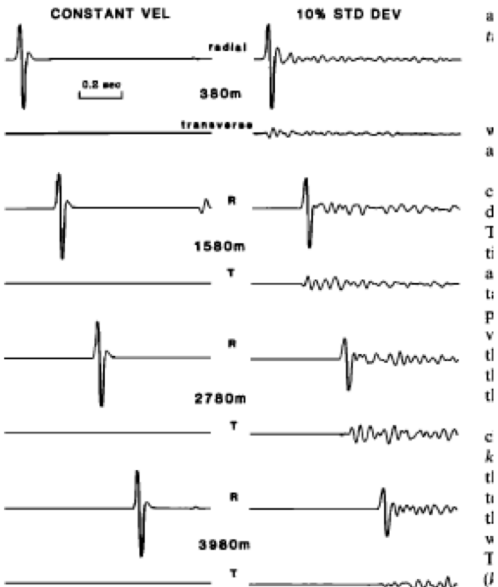


Fig. 4. (Left) Synthetic seismograms for a P wave propagating through a constant velocity medium (see Figure 2 for geometry). Radial and transverse components of velocity are shown for receivers from 380 to 3980 m from the source. Amplitudes of all synthetics shown in this paper are corrected for geometrical spreading. (Right) Synthetic seismograms for a P wave traveling through an exponential random medium ($\sigma_r = 10\%$, $a = 40$ m, $ka = 1.16$ at 30 Hz).

$$\gamma_j^2(\omega) = \int_{\mathbf{x} \in A} \int_{\mathbf{x}' \in A} s_1^*(\mathbf{x}, \omega) C_{11}^j(\mathbf{x}, \mathbf{x}', \omega) s_1(\mathbf{x}', \omega) d\mathbf{x} d\mathbf{x}'$$

To use this equation of the variance γ^2 , we must be able to estimate an accurate spatial covariance function.

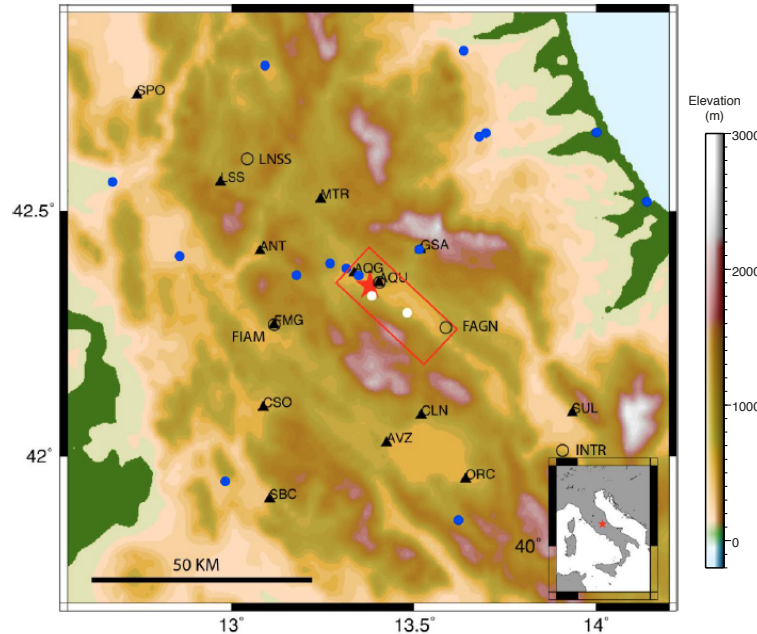
$$C(\mathbf{x}_1, \mathbf{x}_2, \omega) \propto f(|\mathbf{x}_1 - \mathbf{x}_2|, \omega)$$

There are two possibilities:

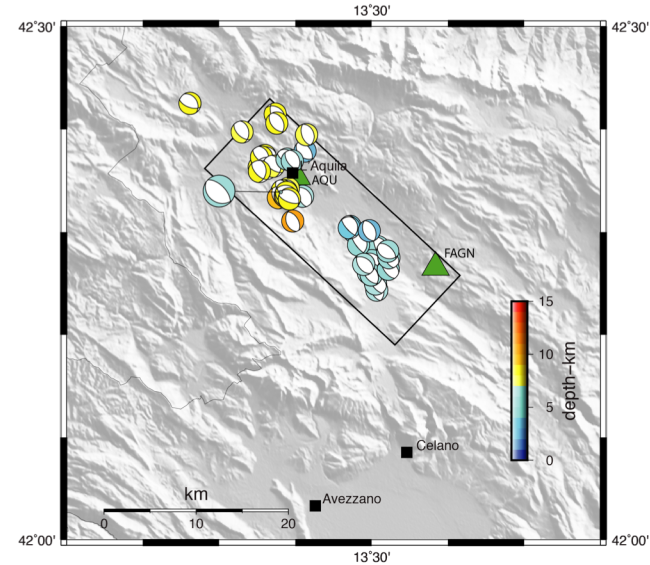
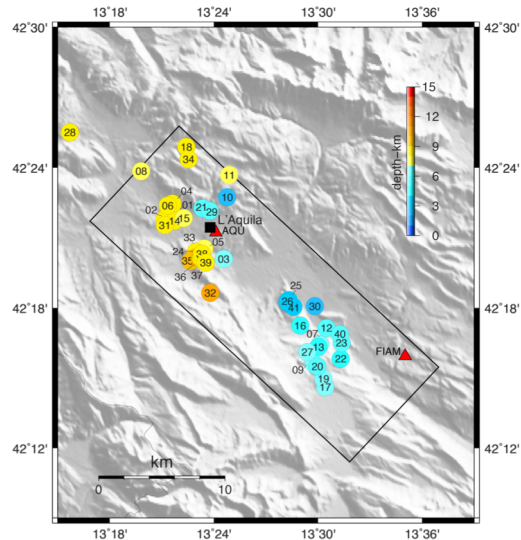
- 1) If you have recordings of many small earthquakes on the rupture surface of interest, you can treat them as empirical Green's functions and use them to calculate the error in your theoretical Green's functions.
- 2) If you do not have recordings of many empirical Green's functions, it might be possible to infer the needed spatial covariances, following Frankel and Clayton (JGR, 1986), from coda-Q and teleseismic travel-time and amplitude anomalies.

We have selected for study the 6 April 2009 M6.1 L'Aquila, central Italy, earthquake and its **on-fault** aftershocks, from which we derive covariance function

Map of strong motion and other stations

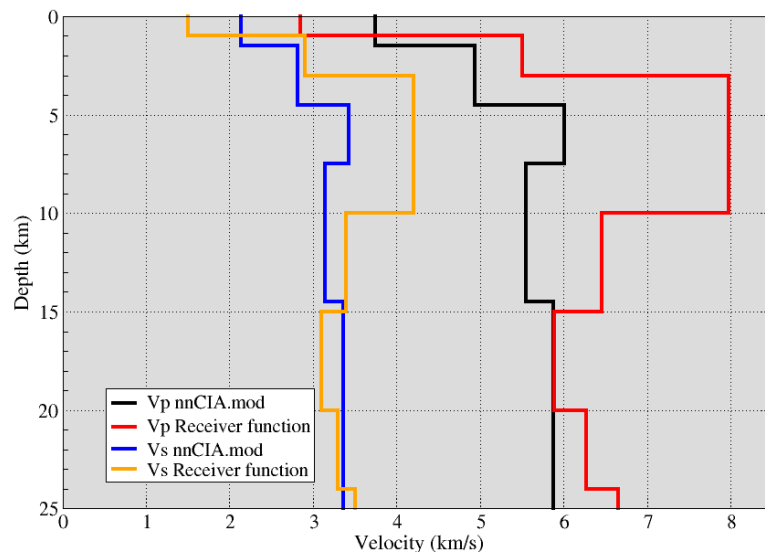


Selected aftershock locations and mechanisms



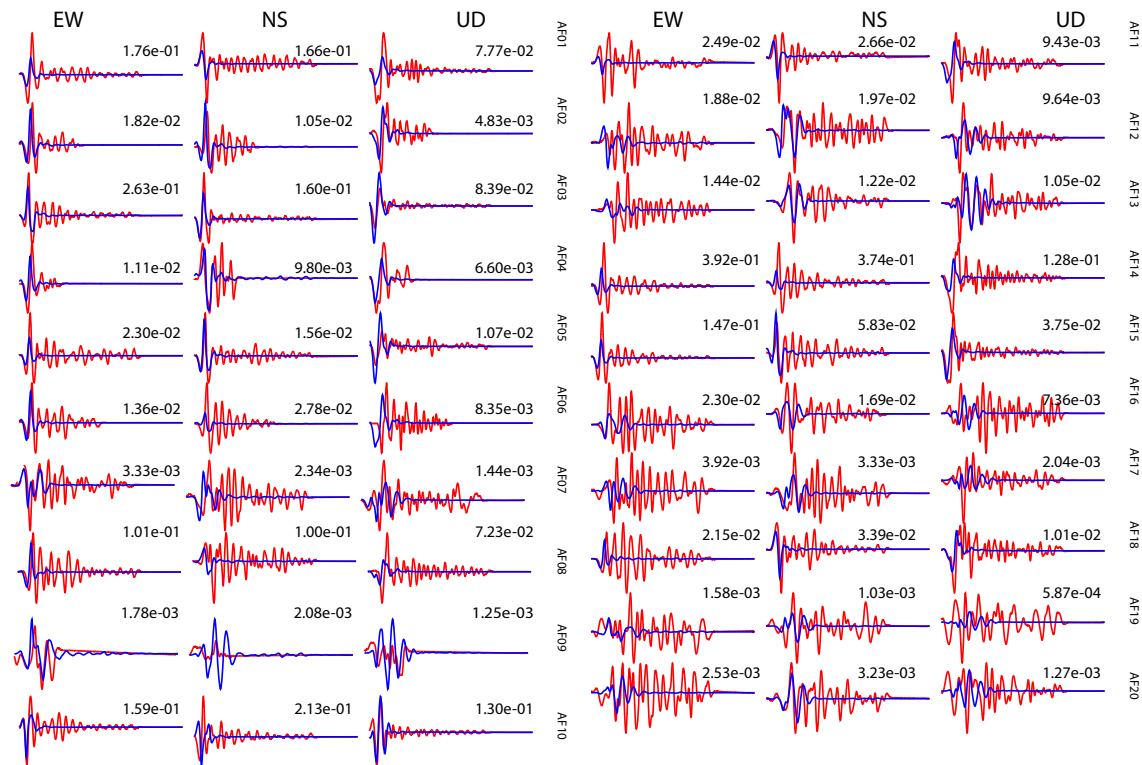
We chose as empirical Green's functions 37 events recorded by AQU and FIAM seismic stations which have M_w between 2.3 and 3.8, high signal to noise ratio, and focal planes within 30 degrees of the main shock mechanism

Two different seismic velocity structures, **CIA model**, shown by the black and blue curves, and the **receiver function (RF) model**, shown by the red and orange curves, were used to calculate point source synthetics at AQU and FIAM for these aftershocks.



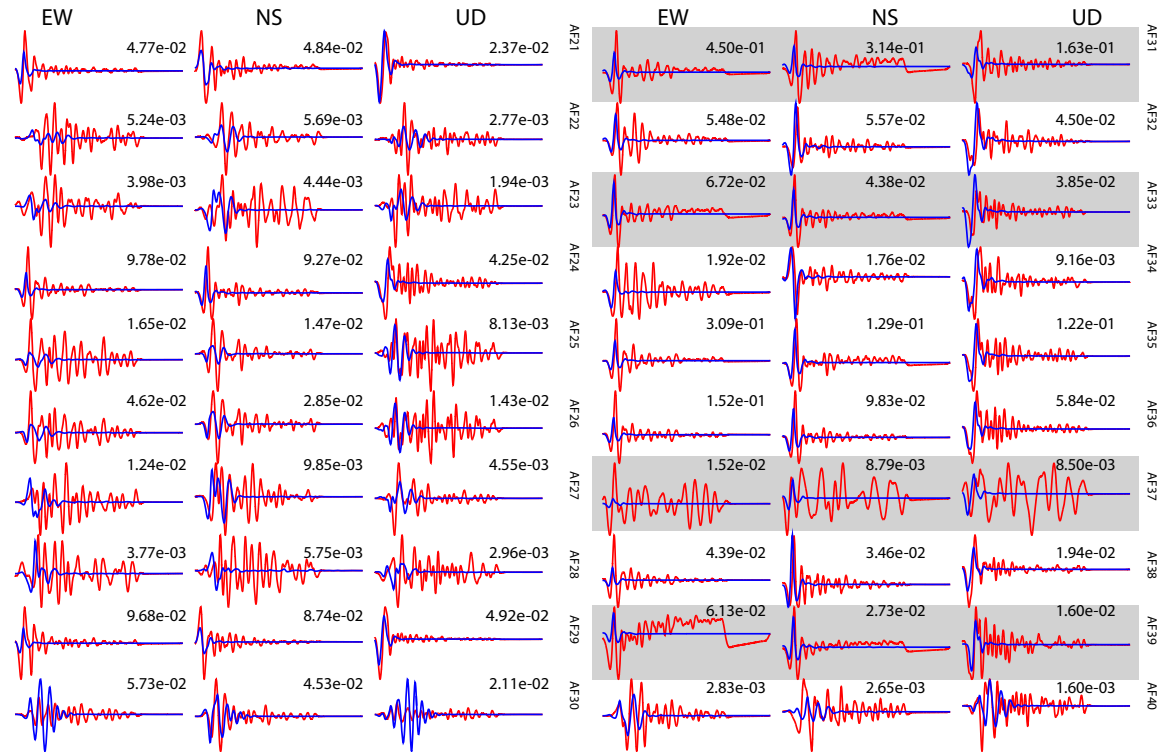
Forward models for point sources whose moment tensor solutions have been inferred from farther broadband stations at lower frequency band.

Observed ground velocity at **AQU** (red) and synthetic velocity (blue) for the RF structure for frequency band 0.02-0.5 Hz. Number is peak velocity of data seismogram. First 40s of total 60s seismograms are shown.

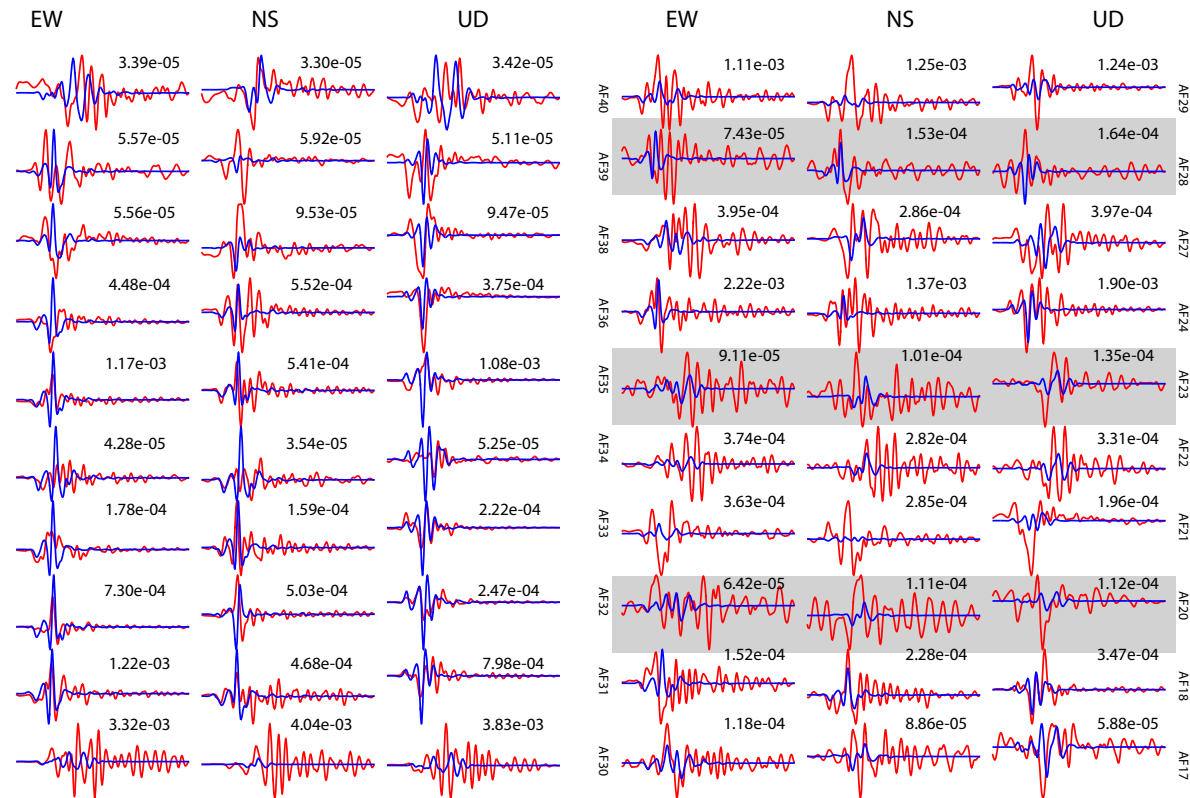


Observed ground velocity at **AQU** (red) and synthetic velocity (blue) for the RF structure, plotted at the same scale as the observations.

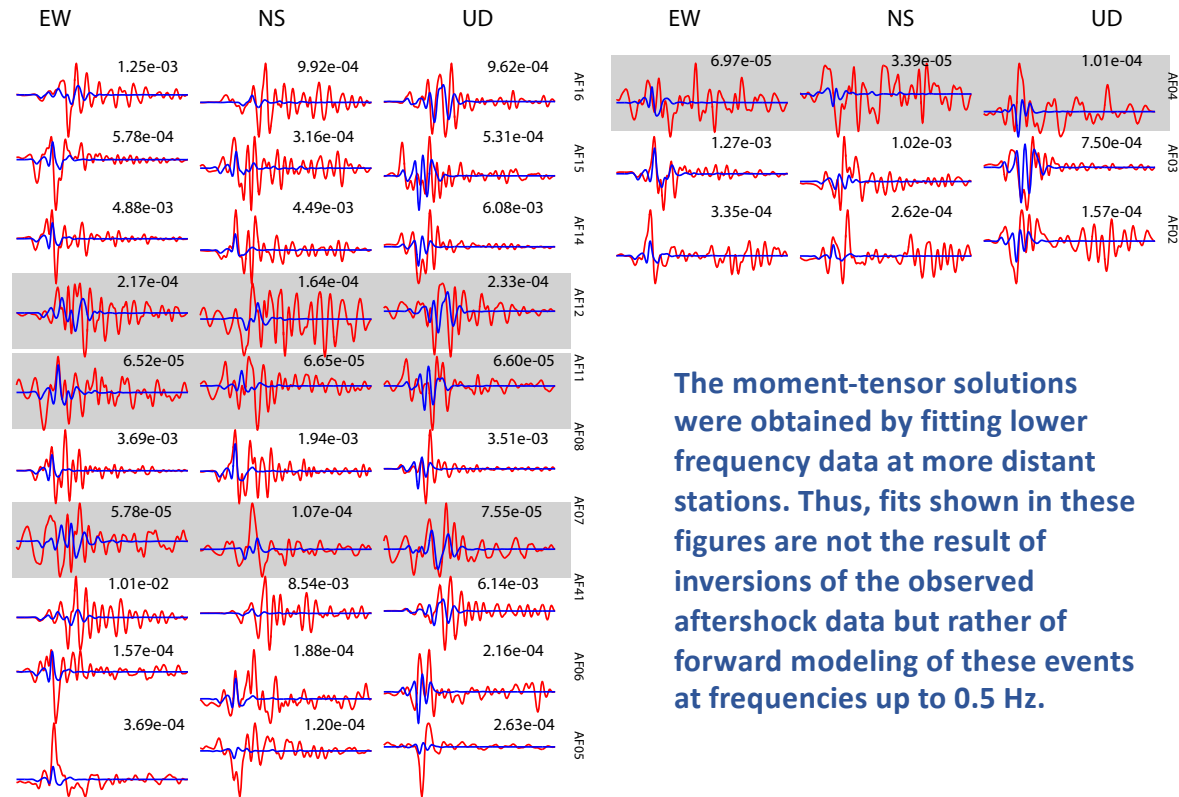
We removed from the analysis those data for which the observed data had obvious ground noise or processing glitches



Observed ground velocity at **FIAM** (red) and synthetic velocity (blue) for the CIA structure, plotted at the same scale as the observations, for a subset of the aftershocks. Number is peak velocity of data seismogram. First 40s of total 60s seismograms are shown.



Observed ground velocity at **FIAM** (red) and synthetic velocity (blue) for the CIA structure, plotted at the same scale as the observations, for a subset of the aftershocks. Number is peak velocity of data seismogram. First 40s of total 60s seismograms are shown.



The moment-tensor solutions were obtained by fitting lower frequency data at more distant stations. Thus, fits shown in these figures are not the result of inversions of the observed aftershock data but rather of forward modeling of these events at frequencies up to 0.5 Hz.

Recovering traction from ground velocity

$$C_{11}^j(\mathbf{x}_1, \mathbf{x}_2, \omega) = E[\delta g_1^{j*}(\mathbf{x}_1) \delta g_1^j(\mathbf{x}_2)]$$

For each frequency and component of motion we form the complex difference

$$\Delta_i^j = v_i - s_i^j$$

s_i is the aftershock synthetic

v_i is the observed aftershock datum, which is the product of a moment times the Green's function divided by a rigidity.

$$v_i = \frac{M_i}{\mu_i} g_i$$

The **complex difference** for each frequency and component is then

$$\Delta_i^j = v_i - s_i^j = v_i - P_i^j g_i^j.$$

Where \tilde{P}_i^j be our j th incorrect estimate of $\frac{M_j}{\mu_i}$

Normalizing by seismic moment and rigidity yields a quantity with the units of the traction Green's function, namely the **scaled complex difference** (or equivalently the **empirical traction error**)

$$\Delta_i^j = \left(c \Delta_i^j / P_i^j \right) = \left(\frac{v_i}{P_i^j} - g_i^j \right) c$$

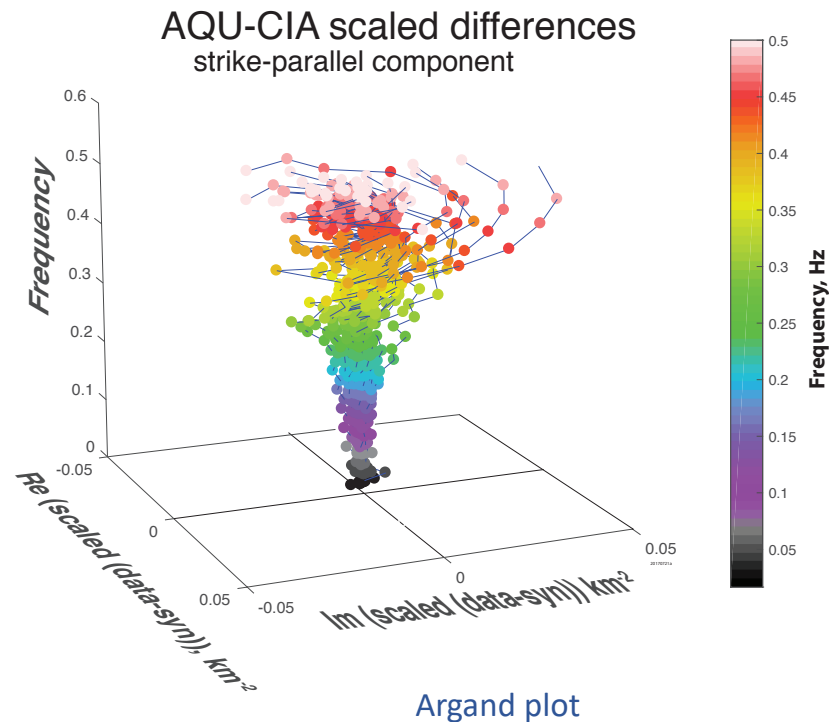
Unit of this empirical traction error are km^{-2} . the units of covariance of the errors in Fourier transform is km^{-4} .

We need to
compute error in
green function unit

Empirical traction errors differences in the complex plane for **AQU** station using **CIA** model

They show that the empirical traction errors grow in magnitude as frequency increases, justifying the appropriateness of our frequency-domain approach.

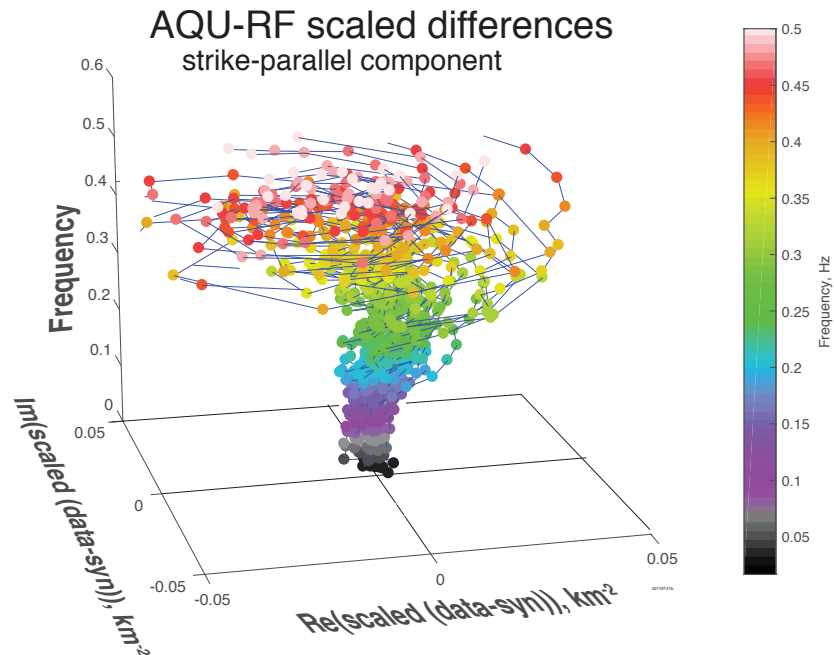
The colored dots showing the empirical traction errors for a particular aftershock are strung together with a black line



Empirical traction errors differences in the complex plane for **AQU** station using **RF model**

For many aftershocks the empirical traction errors form expanding helices, corresponding to progressive phase shifts as a function of frequency

We have not introduced 'static corrections' into the theoretical Green's functions to remove these time mismatches because time mismatches are errors in the theoretical Green's functions, the effect of which we hope to quantify



The covariance between the empirical traction at \mathbf{x}_i and \mathbf{x}_k for component of motion j and frequency index n is

$$K_{ik}^j(\omega_n) = C_{11}^j(\mathbf{x}_i, \mathbf{x}_k, \omega_n) = E\left[\delta g_1^j(\mathbf{x}_i, \omega_n)^* \delta g_1^j(\mathbf{x}_k, \omega_n)\right] = E\left[\Delta^j(\mathbf{x}_i, \omega_n)^* \Delta^j(\mathbf{x}_k, \omega_n)\right]$$

we omit the slip direction indices entirely as the aftershock rakes are chosen to be within 30 degrees of the dominant slip direction

$$K_{ik}^j(\omega_n) = C_{11}^j(\mathbf{x}_i, \mathbf{x}_k, \omega_n) = E\left[\delta g_1^j(\mathbf{x}_i, \omega_n)^* \delta g_1^j(\mathbf{x}_k, \omega_n)\right] = E\left[\Delta^j(\mathbf{x}_i, \omega_n)^* \Delta^j(\mathbf{x}_k, \omega_n)\right]$$

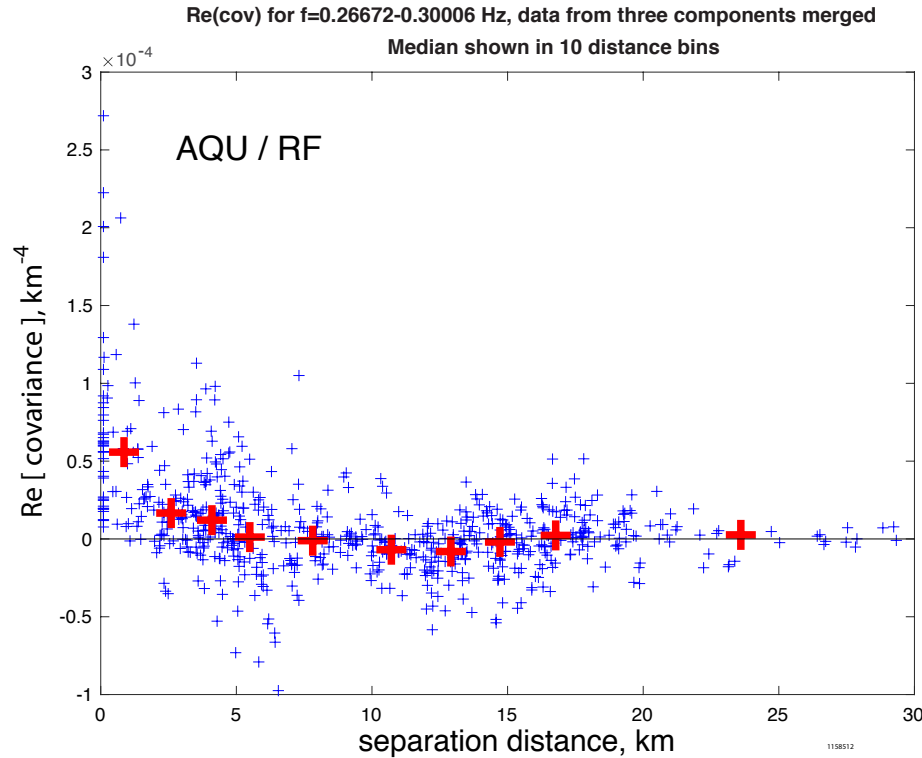
To take the expected value, we average the above over all three components of motion j and over a frequency band of three adjacent frequencies n :

$$C(\mathbf{x}_i, \mathbf{x}_k, \omega_{n_o}) = \frac{1}{3} \sum_{j=1}^3 \frac{1}{3} \sum_{n=n_o}^{n_o+2} \text{Re}\left(\hat{\Delta}^j(\mathbf{x}_i, \omega_n)^* \hat{\Delta}^j(\mathbf{x}_k, \omega_n)\right)$$

We call each value of $C(\mathbf{x}_i, \mathbf{x}_k, \omega_{n_o})$

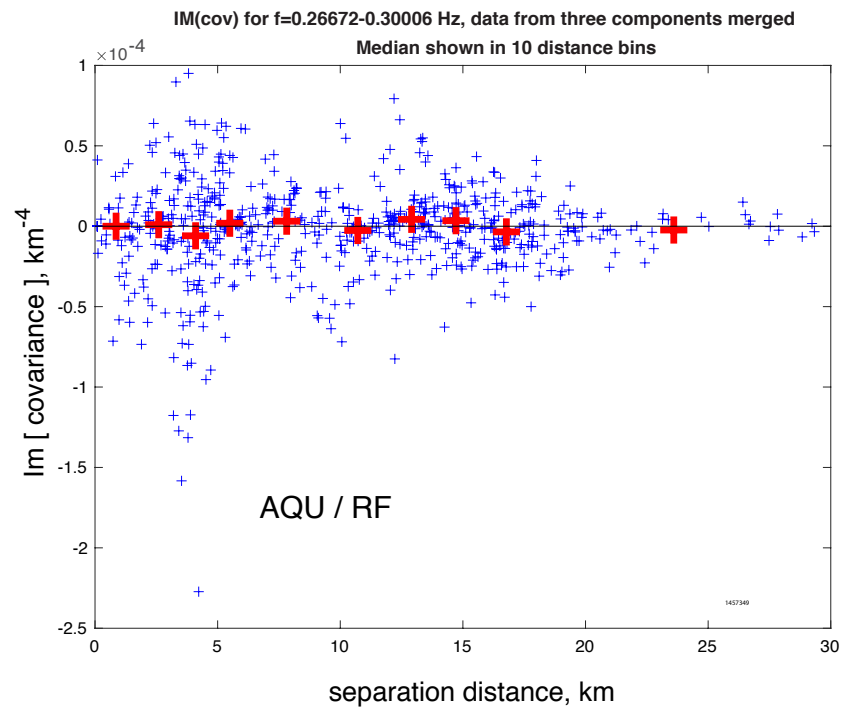
a covariance datum, and in the next slide we plot all the covariance data for a single station and frequency band n_o as a function of separation

$$r = |\mathbf{x}_i - \mathbf{x}_k|$$



Blue dots: Example of the real part of the Covariance data for a fixed small frequency band.

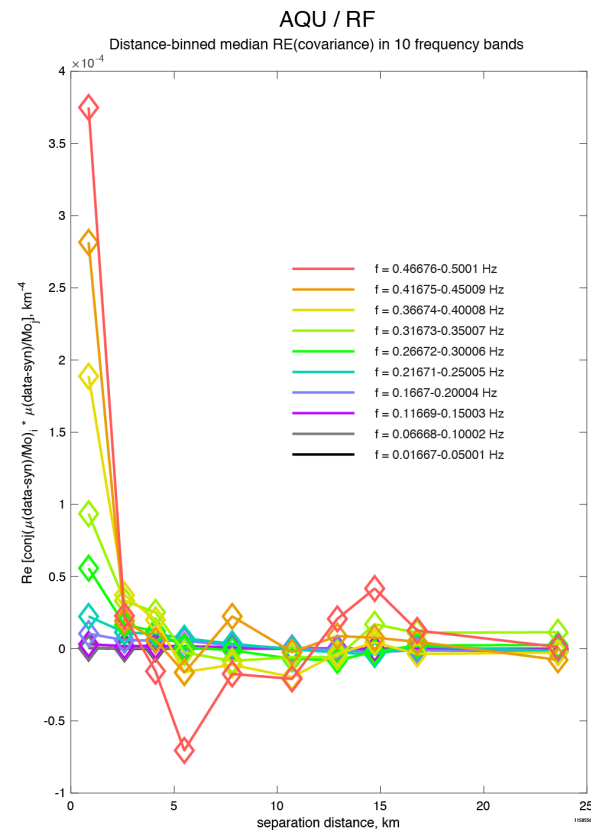
Red crosses: median values in each of 10 separation distance bins (in each bin there are about 70 covariance data).



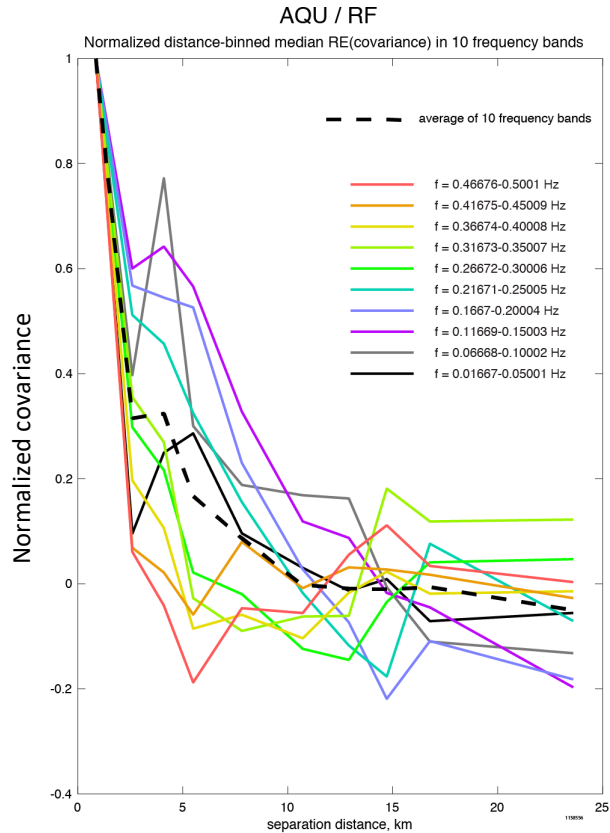
The median of the imaginary part of the covariance data is not significantly different from zero

AQU COVARIANCE FUNCTIONS FOR ALL STUDIED FREQUENCIES

Covariance functions for
10 frequency bands at
AQU using the RF velocity
structure

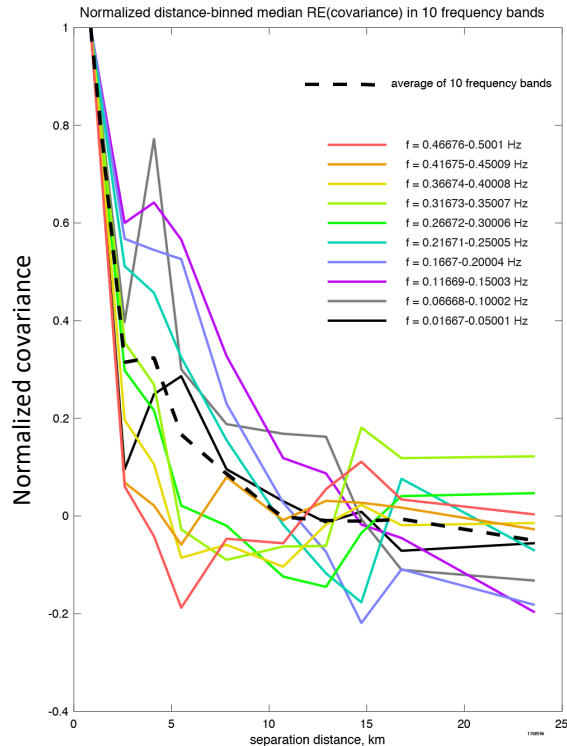


NORMALIZED COVARIANCE FUNCTIONS FOR ALL STUDIED FREQUENCIES

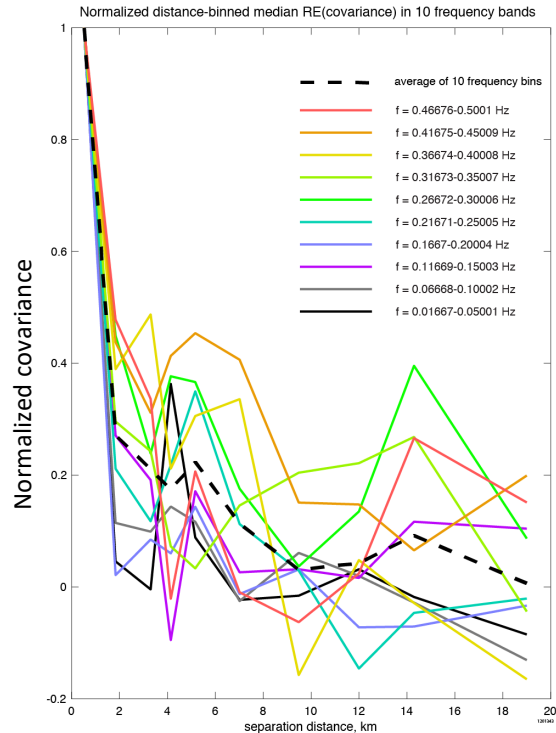


NORMALIZED COVARIANCE FUNCTIONS FOR ALL STUDIED FREQUENCIES

AQU + RF model

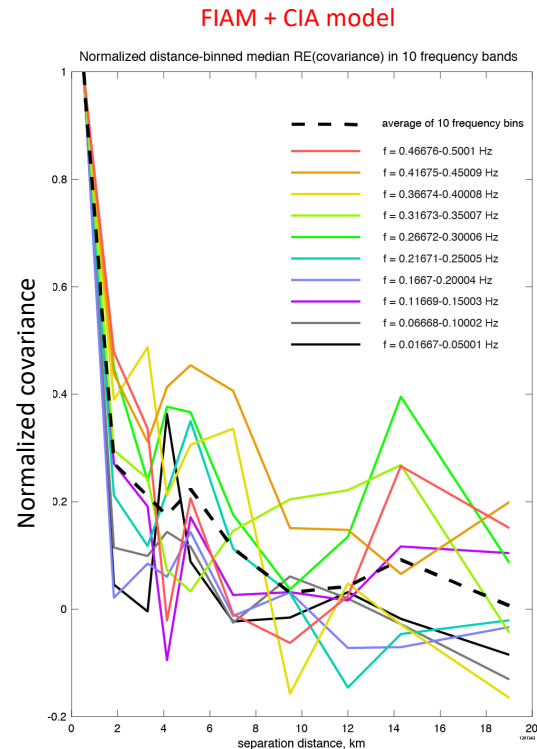
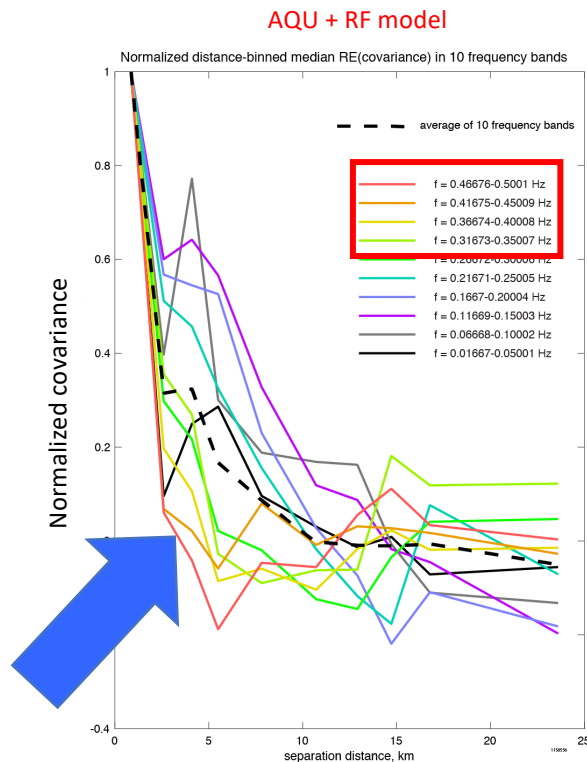


FIAM + CIA model



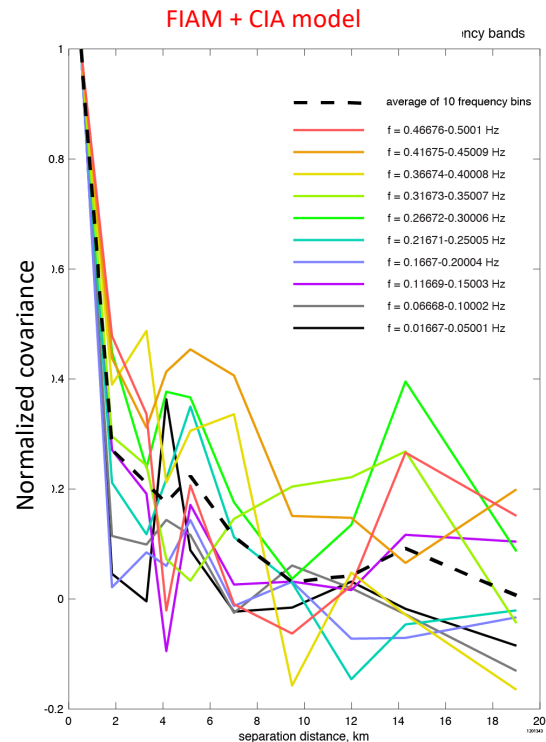
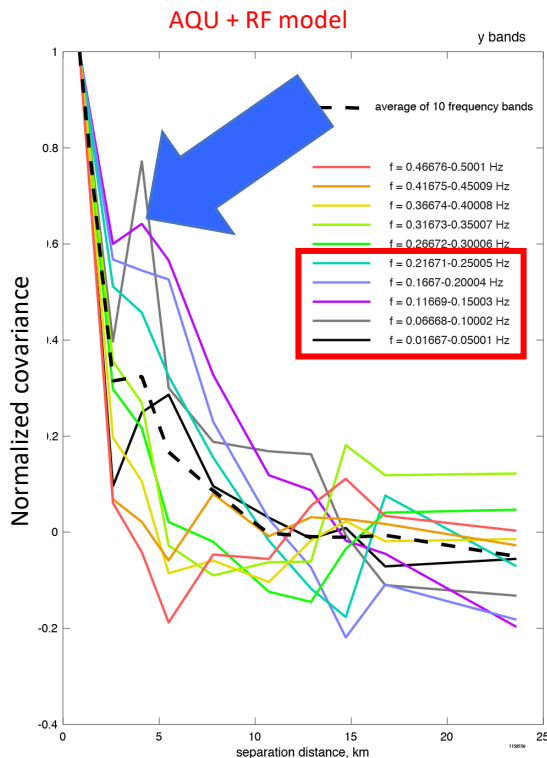
The dashed average covariance functions are similar in shape to Frankel and Clayton (1986) covariance functions for exponential and self-similar media, although our covariance functions suggest a covariance distance less than their 10 km.

NORMALIZED COVARIANCE FUNCTIONS FOR ALL STUDIED FREQUENCIES

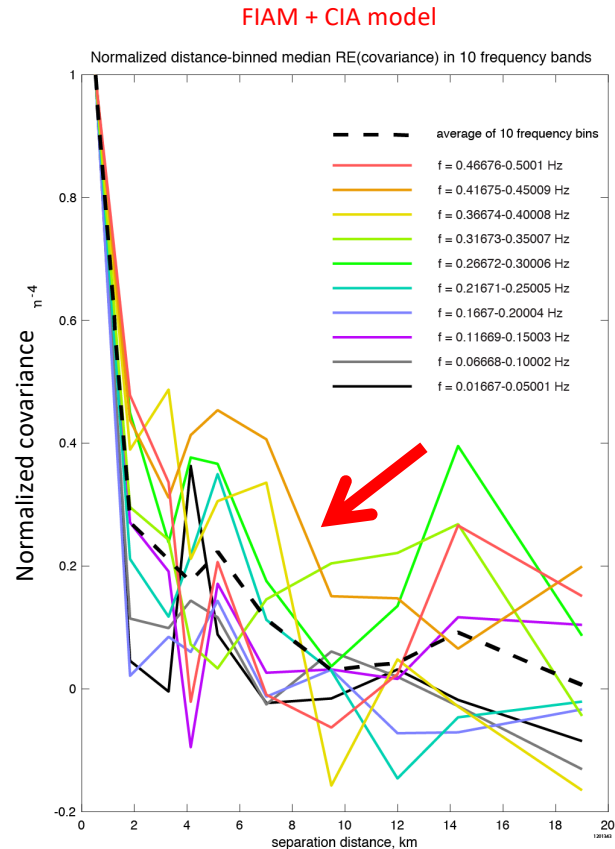
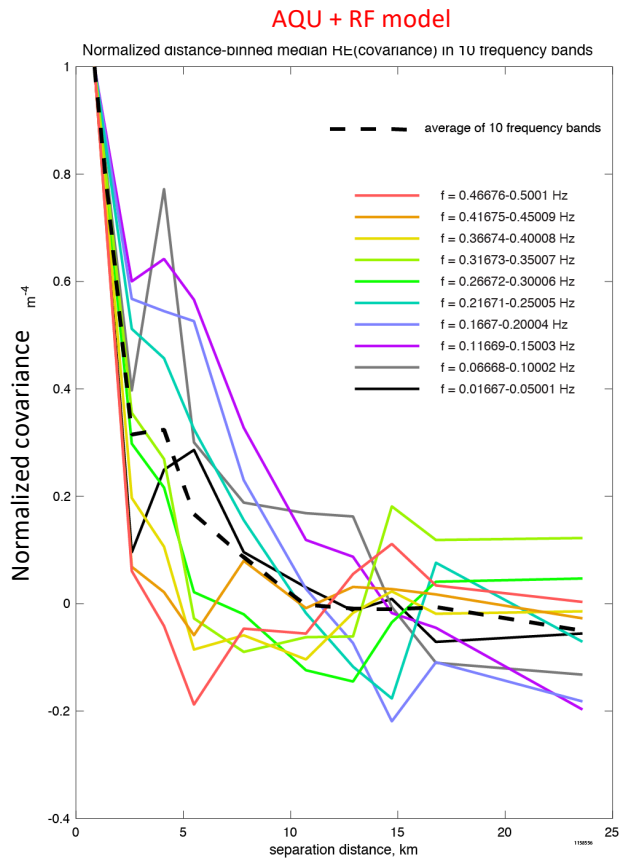


the high frequency covariance functions (red, orange, yellow, and green) lying below the dashed average.

NORMALIZED COVARIANCE FUNCTIONS FOR ALL STUDIED FREQUENCIES



the low frequency data (blue, purple, gray, and black)
lie above the dashed average



no frequency
dependence
is seen on
the right
panel for
FIAM

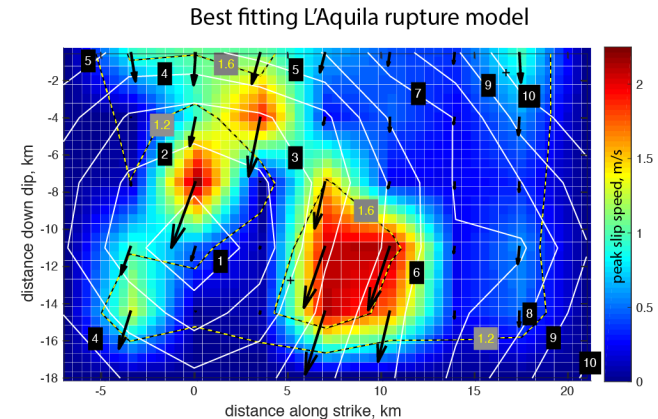
We evaluate γ^2 for a specific rupture model of the L'Aquila earthquake, namely the minimum cost model found by Cirella et al. (2009)

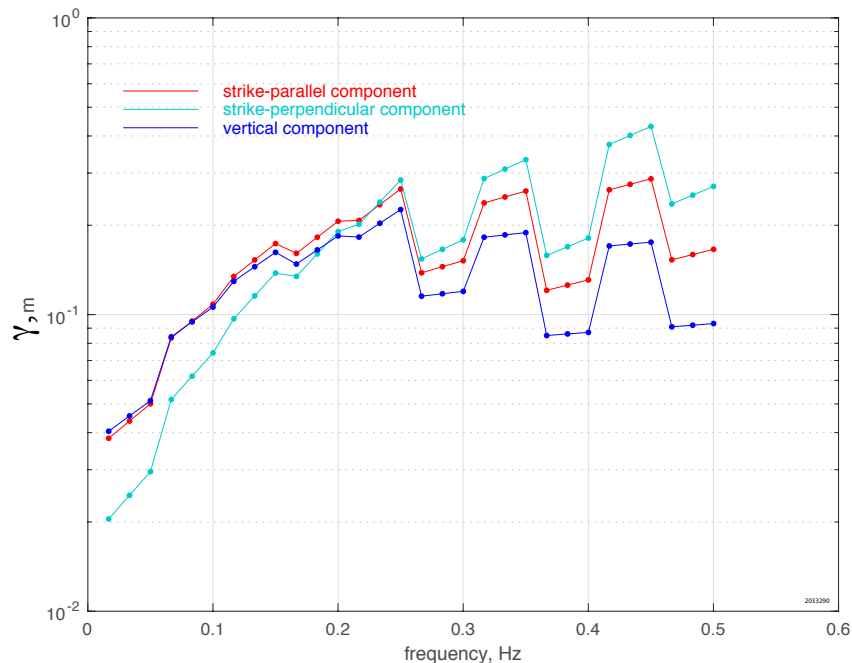
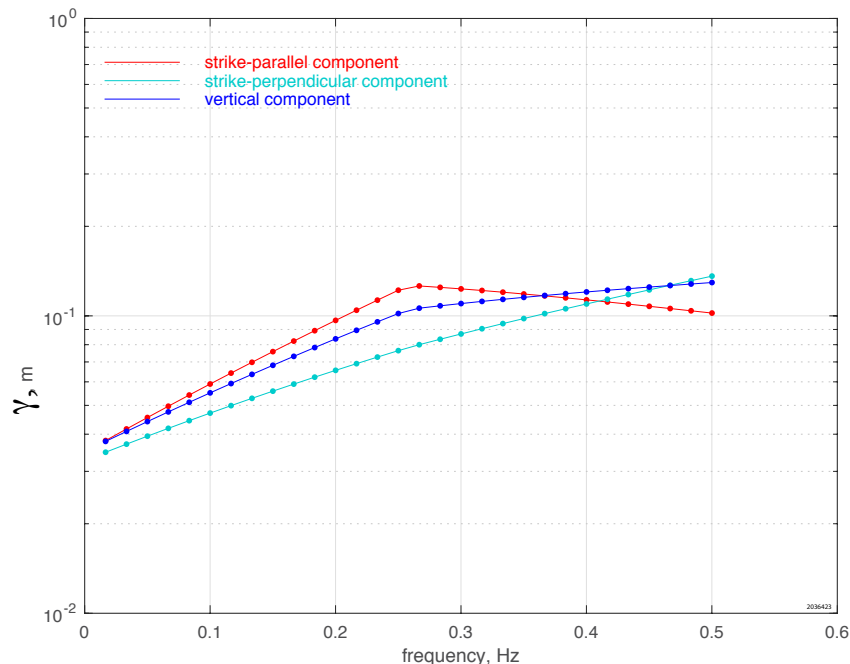
$$\gamma_{sc}^2(\omega) = \int_{\mathbf{x} \in A} \int_{\mathbf{x}' \in A} s_1^*(\mathbf{x}, \omega) K^{sc}(r, \omega) s_1(\mathbf{x}', \omega) d\mathbf{x} d\mathbf{x}'$$

where

- j is the channel number, a single component of motion at a single station
- A is the rupture area.

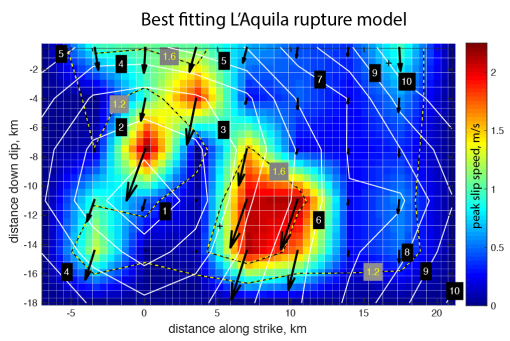
We developed a continuous empirical covariance function $K(r, \omega)$ to insert into the equation. Because FIAM resulted frequency independent we adopt the dashed average correlation while for AQU we adopt each individual colored function.



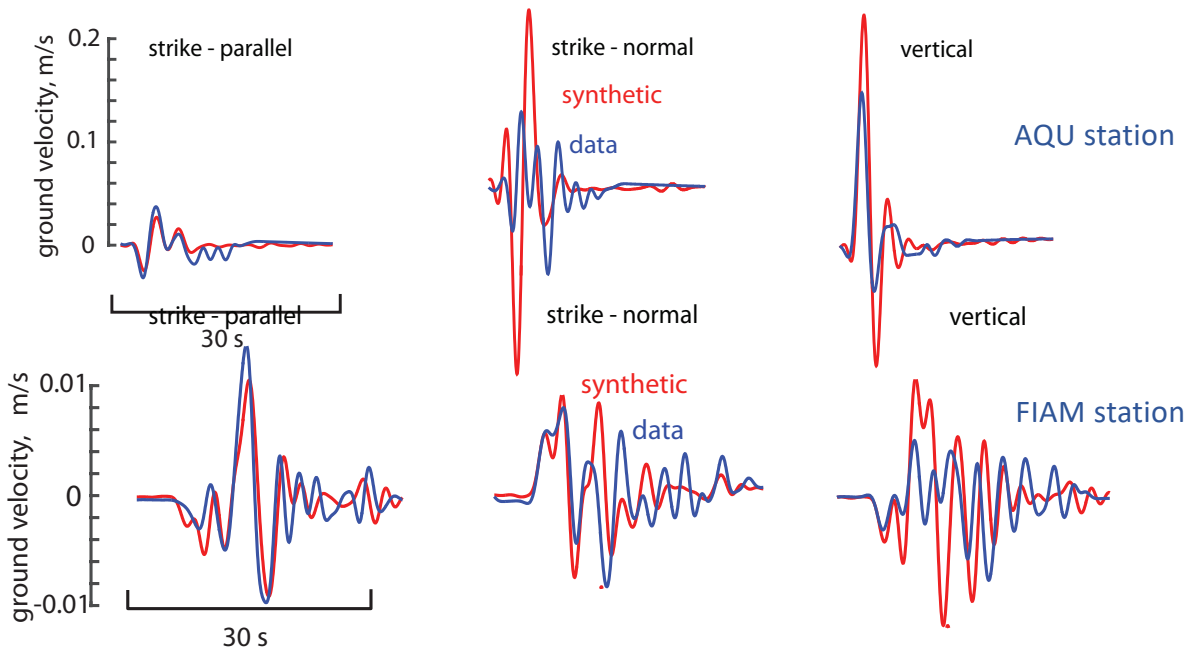
The resulting standard deviation γ (square root of real γ^2) spectra for all components γ for AQU / RF - frequency dependent covariance functions γ for FIAM / CIA

The alternately depressed and elevated spectral levels are caused by use of the individual colored linear median covariance functions

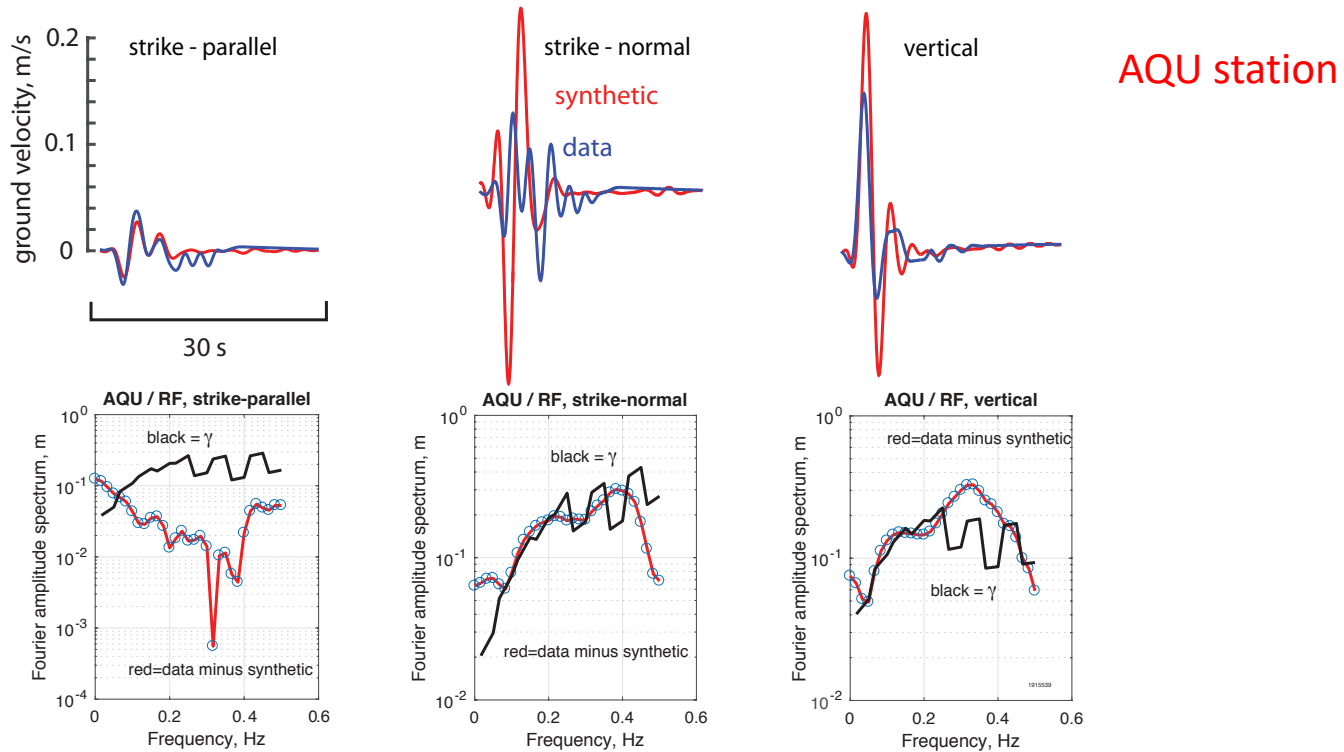
Now we can compare the main shock data-minus-synthetic misfit with γ , the misfit expected from green's function errors.



Fit of the Mw=6.1
2009 L'Aquila event
for frequency 0.02-
0.5 Hz



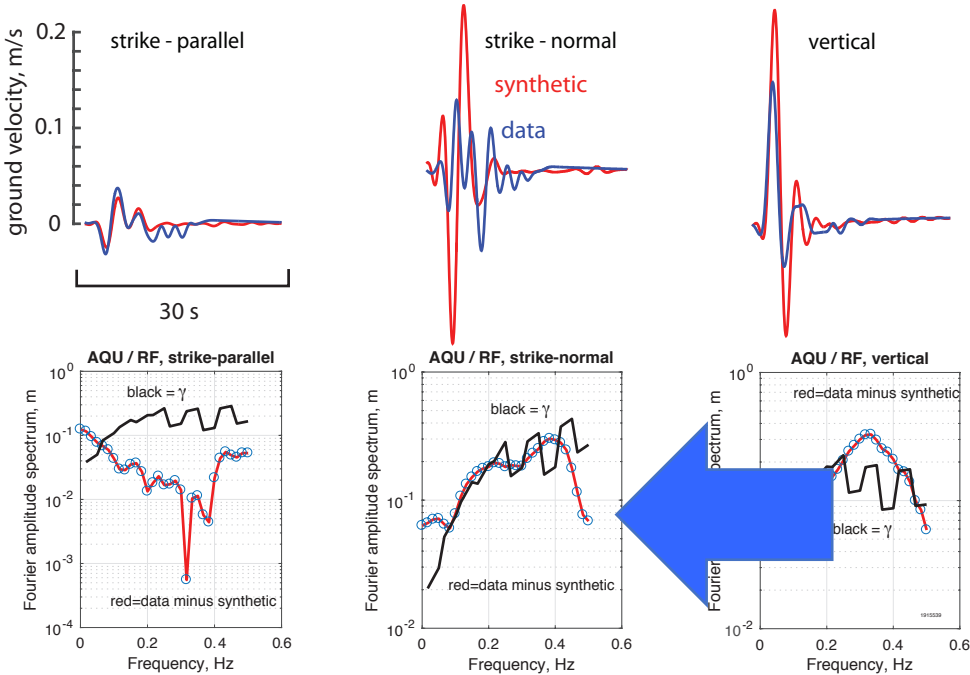
Comparison of data-synthetic misfits with γ for AQU / RF



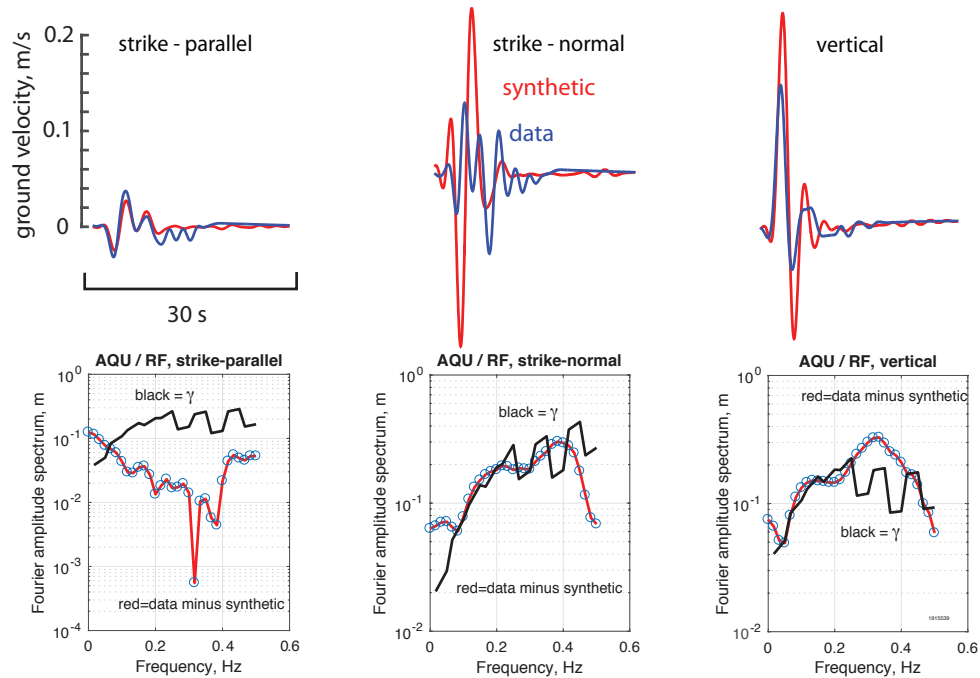
Comparison of data-synthetic misfits with γ for AQU / RF

AQU station

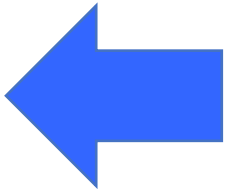
The agreement of the γ spectrum with the red misfit tells us that the misfit we see in the seismogram is consistent with the misfit expected



Comparison of data-synthetic misfits with γ for AQU / RF



AQU station

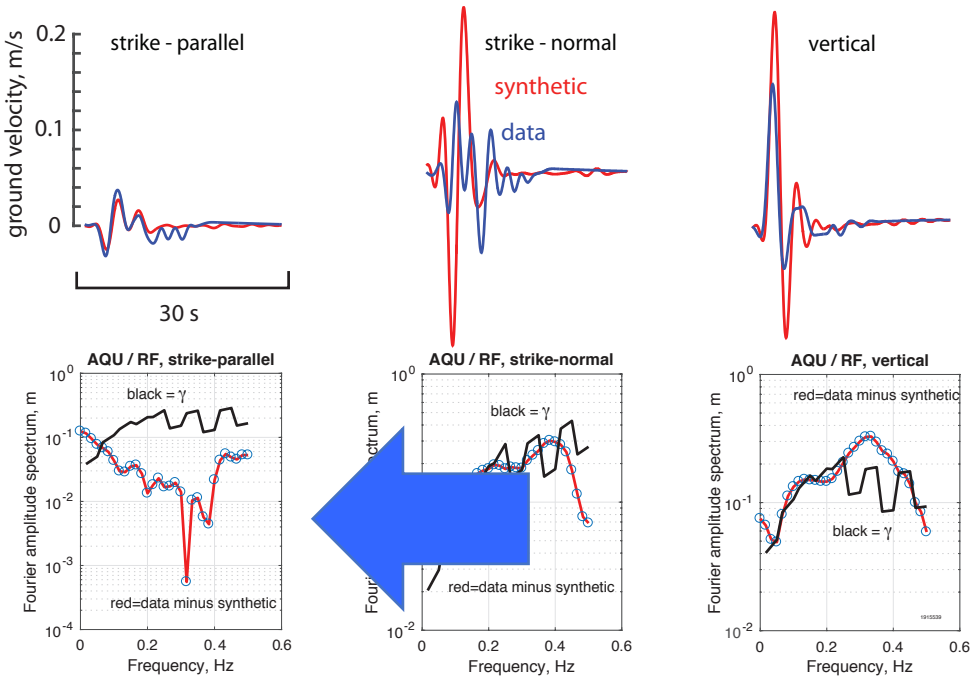


The γ spectrum lies below the red misfit from 0.25 – 0.45 Hz: the seismogram is underfit.

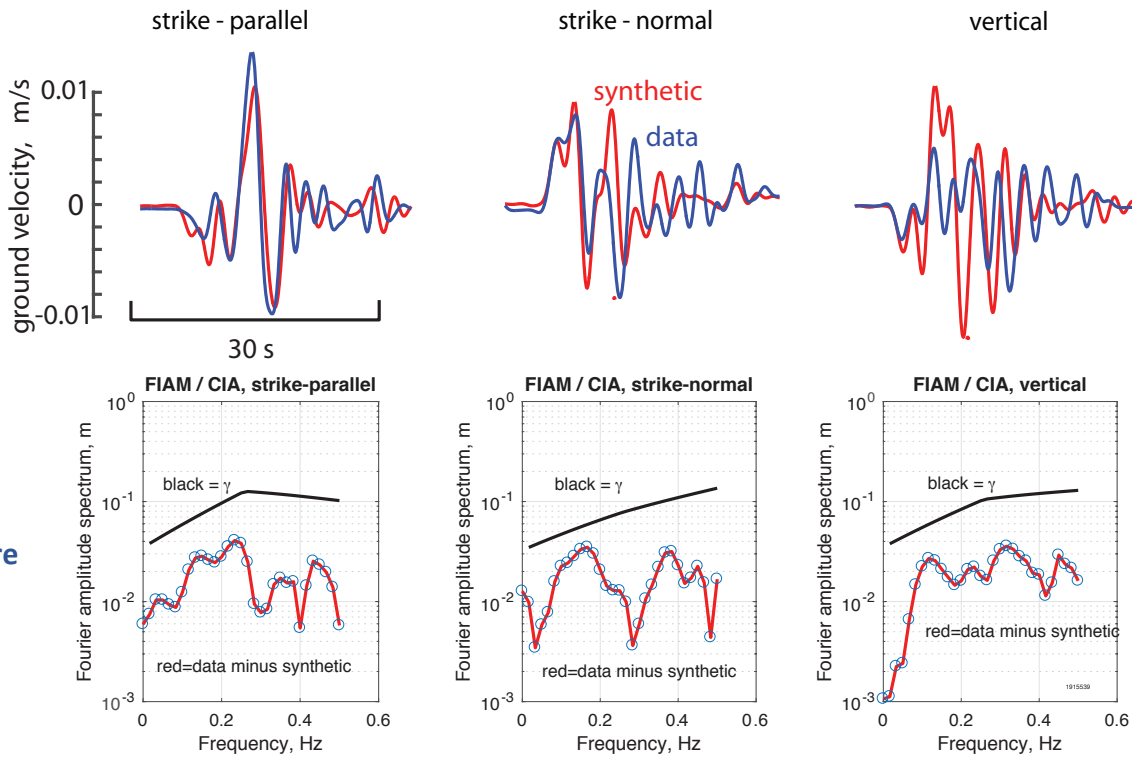
Comparison of data-synthetic misfits with γ for AQU / RF

AQU station

Strike – parallel component are **over-fit**: it shows an excessively good fit to the data considering the non-negligible theory errors.



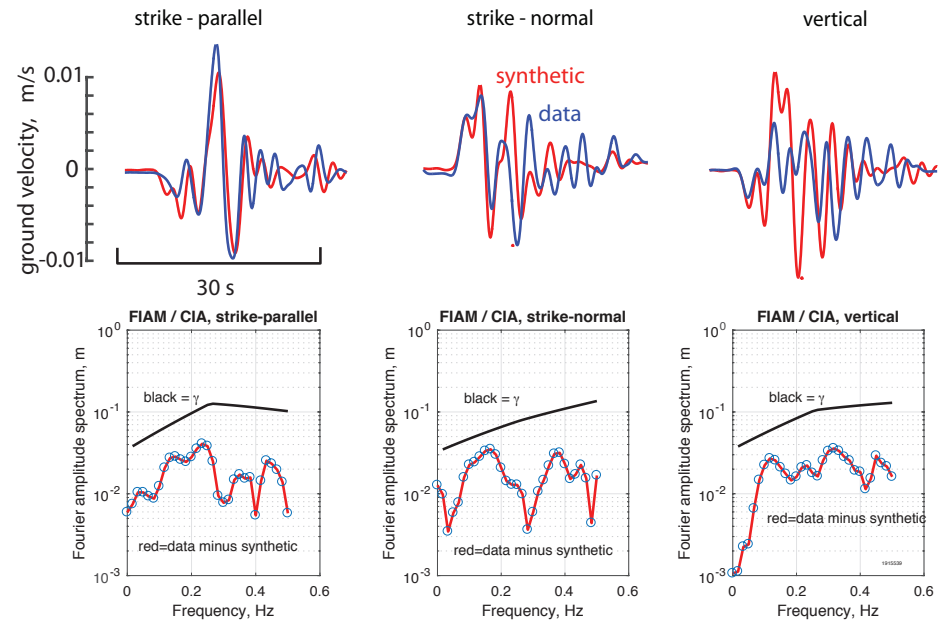
Comparison of data-synthetic misfits with γ for FMG / CIA



These error estimates are very disturbing. Most investigators would consider the waveform fit of the all components at FMG as being good fits.

If these error estimates are correct and representative of typical errors in rupture inversions using numerical Green's functions, it implies that the slip models of the many rupture models derived from past earthquakes are much less well resolved than currently thought.

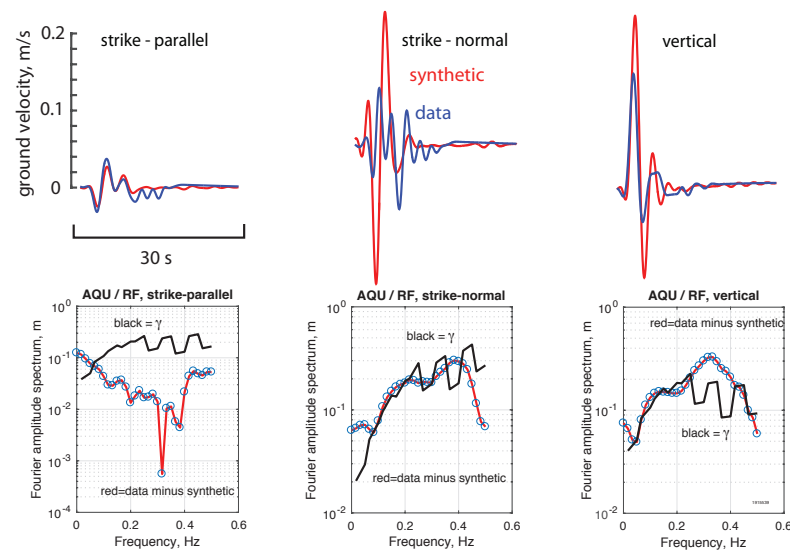
Comparison of data-synthetic misfits with γ for FMG / CIA



SUMMARY – 1

Are ground motion inversions corrupted by Green's function errors? May we have computed to excessively large γ ?

One might argue that our comparison of Green's functions to aftershock waveforms is quite bad; for example, there is no hope of fitting the aftershock codas.

Comparison of data-synthetic misfits with γ for AQU / RF

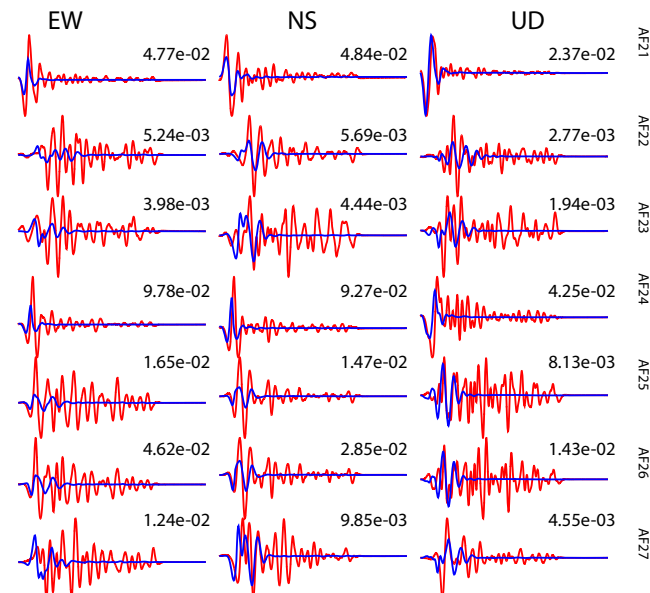
SUMMARY – 1

Are ground motion inversions corrupted by Green's function errors? May we have computed to excessively large γ ?

One might argue that our comparison of Green's functions to aftershock waveforms is quite bad; for example, there is no hope of fitting the aftershock codas.

However, the observed main shock seismograms contain the codas of early rupturing parts of the rupture, so it is necessary to consider the codas in the aftershock modeling.

No measurement of Green's function error is typically done for crustal earthquakes, so it might be that rather than being *catastrophically bad*, our comparison is one of the best achievable.



Two other sources of variability in earthquake ground velocity

$$v_j(\omega, \mathbf{y}) = \int_{\mathbf{x} \in A} \mathbf{s} \cdot \mathbf{g}^{(j)} dA + \int_{\mathbf{x} \in A} \delta \mathbf{s} \cdot \mathbf{g}^{(j)} dA + \int_{\mathbf{x} \in A} \mathbf{s} \cdot \delta \mathbf{g}^{(j)} dA + \int_{\mathbf{x} \in A} \delta \mathbf{s} \cdot \delta \mathbf{g}^{(j)} dA.$$



the ground velocity
caused by perturbations
of the rupture model



the ground velocity caused
by joint perturbations of
the rupture model and
errors in the Green's
functions

The variability in ground velocity of the j -th channel (single component of motion at a particular observation location) caused by perturbations of the rupture model has the following variance:

$$\delta v_j^s = \int_{\mathbf{x} \in A} \delta \mathbf{s} \cdot \mathbf{g}^{(j)} dA$$

$$\rho_j^2(\omega) = \int_{\mathbf{x} \in A} \int_{\mathbf{x}' \in A} g_1^{(j)*}(\mathbf{x}, \omega) S_{11}(\mathbf{x}, \mathbf{x}', \omega) g_1^{(j)}(\mathbf{x}', \omega) d\mathbf{x} d\mathbf{x}'$$

It depends on the spatial covariance of perturbations of the rupture model S_{11}

$$\mathbf{S}(\mathbf{x}, \mathbf{x}', \omega) = E \begin{bmatrix} \delta s_1^*(\mathbf{x}) \delta s_1(\mathbf{x}') & \delta s_1^*(\mathbf{x}) \delta s_2(\mathbf{x}') \\ \delta s_2^*(\mathbf{x}) \delta s_1(\mathbf{x}') & \delta s_2^*(\mathbf{x}) \delta s_2(\mathbf{x}') \end{bmatrix}$$

The variability in ground velocity of the j -th channel (single component of motion at a particular observation location) caused by perturbations of the rupture model has the following variance:

$$\delta v_j^s = \int_{\mathbf{x} \in A} \delta \mathbf{s} \cdot \mathbf{g}^{(j)} dA$$

$$\rho_j^2(\omega) = \int_{\mathbf{x} \in A} \int_{\mathbf{x}' \in A} g_1^{(j)*}(\mathbf{x}, \omega) S_{11}(\mathbf{x}, \mathbf{x}', \omega) g_1^{(j)}(\mathbf{x}', \omega) d\mathbf{x} d\mathbf{x}'$$

It depends on the spatial covariance of perturbations of the rupture model S_{11}

Future applications

- The primary use will be in seismic hazard studies to calculate the variability of synthetic seismograms given an ensemble of rupture models
- The variance of the ground motion is determined directly, skipping the step of calculating the ground motions of many rupture models.

Variability of the ground velocity
due to the interaction between δs
and δg has the following variance:

$$\delta v_j^{sg} = \int_{\mathbf{x} \in A} \delta \mathbf{s} \cdot \delta \mathbf{g}^{(j)} dA = \int_{\mathbf{x} \in A} \left(\delta s_1 \delta g_1^{(j)} + \delta s_2 \delta g_2^{(j)} \right) dA$$

$$\xi_j^2(\omega) = \int_{\mathbf{x} \in A} \int_{\mathbf{x}' \in A} \text{Cov} \left[\delta s_1(\mathbf{x}') \delta g_1^{(j)}(\mathbf{x}'), \delta s_1(\mathbf{x}) \delta g_1^{(j)}(\mathbf{x}) \right] d\mathbf{x} d\mathbf{x}'$$

Future applications

The possibility of a nonzero covariance between δs and δg in the error interaction term opens an interesting line of research. We can imagine that spatial variations of rigidity in the fault zone might cause spatial variations of δg . These spatial variations of rigidity might also cause correlated variations in the rupture process δs . It would be very interesting to look for such correlations in numerical simulations of spontaneous rupture in heterogeneous media.

This expression is new to seismic hazard research, because δs and δg might not be small this variance can be significant

SUMMARY – 2

We have found a simple equation relating the variance in the ground motions predicted from a given slip model to the spatial covariance function of the Green's function errors.

This variability would be considered to be epistemic, as it is caused by unknowns in the Earth structure, which could be improved by collection of more data.

The spatial covariance function of Green's function errors can be recovered from analysis of small earthquakes (like aftershocks) spanning the rupture surface.

For regions with sparse seismicity, it might be possible to define a spatial covariance function from study of teleseismic amplitude and travel-time variations, and from coda-Q.

SUMMARY – 3

We have computed the expected variance (and the standard deviation) of ground motion variations due to Green's function errors for the Mw=6.1 2009 L'Aquila earthquake;

We have compared the inferred standard deviation with the misfit of synthetic and real data for the Mw=6.1 2009 L'Aquila earthquake and we have discussed/discovered which are the data over-fitted by the slip model.

SUMMARY – from LITERATURE (Yagi and Fukuhata 2011, Minson et al 2013-2014, Duputel et al. 2012-2014...)

- All the proposed studies develop a model-prediction covariance matrix that accounts for the theory errors;
- These covariance matrix can be use to compute kinematic inversion;
- The improved modelling of C_p is expected to lead to more reliable images of the earthquake rupture, that are more resistant to overfitting of data and include more realistic estimates of uncertainty on inferred model parameters. Duputel et al. suggest that, if more information is available about prior probability density describing the uncertainty of the parameters, another more informative form of PDF can be used.
- This methodology can enable production of the next generation of source models that are more resistant to over-fitting of data.

SUMMARY – from Spudich et al 2019

- We explicitly accept that the seismic-velocity structure of the medium has random three-dimensional variations on all scales;
- The most general way to characterize these variations is through a statistical model from the spatial covariance based on a combination of observations of empirical Green's functions;
- We use observed aftershock seismograms to derive an empirical spatial-covariance matrix;
- As alternative methodology, instead of adopting a Bayesian approach to derive a kinematic rupture models, we propose to adopt a cost function that is consistent with the covariance (that is, to find rupture models that fit the data within the error bounds given by the variance by using a chi-squared test) and this will reduce significantly the number of explored models.